

CLIMATOLOGY AND ENERGY BUDGET OF THE  
NORTHERN HEMISPHERE  
MIDDLE STRATOSPHERE DURING 1972

WILLIAM R. TAHNK \*\* and  
REGINALD E. NEWELL\*

RESUMEN

La capa atmosférica de 10-2 mb (~30-43 km) recibe en invierno energía de dos fuentes diferentes: energía mecánica es llevada hacia arriba desde la tropósfera y desde la estratósfera baja, mientras que energía es generada *in situ* por los gradientes de calentamientos y enfriamientos radiativos. Demostramos aquí, según datos para 1972, que la última energía gobierna en forma primaria el balance de energía de la estratósfera media al principio del invierno, mientras que la primera llega a ser de tamaño comparable, y a menudo dominante, a la mitad y al final del invierno.

Las fuentes de energía radiactiva para el hemisferio de verano son muy pequeñas, ya que hay considerable compensación entre el calentamiento solar a través de la absorción por ozono y enfriamiento infrarrojo por bióxido de carbono y ozono. Ondas estacionarias y en movimiento aparecen claramente a los 5 y a los 2 mb en invierno, ya que mucho del caos de regiones bajas se filtra en la estratósfera baja; las ondas estacionarias a los 2 mb reflejan propiedades de la superficie más efectivamente que las configuraciones de flujo en niveles más bajos. Una onda moviéndose hacia el oeste, con un período aproximado de un mes se manifestó a principios de 1972.

ABSTRACT

The 10-2 mb (~30-43 km) layer of the atmosphere in winter receives energy from two different sources: mechanical energy is carried up from the troposphere and lower stratosphere while energy is generated *in situ* by the gradients of radiative heating and cooling. We show here from data for 1972 that the latter primarily governs the energy budget of the middle stratosphere in early winter while the former becomes of comparable size, and often dominates, in the middle and late winter.

Radiative energy sources for the summer hemisphere are very small, as there is considerable compensation between solar heating through ozone absorption and infrared cooling by carbon dioxide and ozone. Standing and travelling waves are quite clear-cut at 5 and 2 mb in winter, as much of the chaos of lower regions is filtered out in the lower stratosphere; the standing waves at 2 mb may reflect surface properties more effectively than flow patterns at lower levels. A westward-travelling wave, with a period of about a month, was evident in early 1972.

\*\*Air force Geophysics Laboratory, Bedford, Massachusetts.

\* Department of Meteorology, Massachusetts Institute of Technology, Cambridge, Massachusetts.

## INTRODUCTION

The general circulation of the stratosphere is a subject which has received close scrutiny from those interested in observations of stratospheric wind and temperature fields, from theoreticians and from those who construct numerical models of atmospheric circulations. Fairly early in these studies the first two groups found evidence of strong inter-relationships between the tropospheric and stratospheric circulation; the results from the numerical models have in general confirmed these associations and increased our physical understanding of the processes involved.

When these studies commenced, some twenty years ago, 50mb ( $\sim 21$ km) was the altitude limit of satisfactory data. There has been a gradual extension to higher levels with 25mb and some 10mb ( $\sim 30$ km) coverage in the IGY-IGC period (1957-59) and with maps being drawn at 5mb ( $\sim 36$ km), 2mb ( $\sim 43$ km) and 0.4mb ( $\sim 55$ km) in the IQSY period (1964-65). Initially these higher level analyses were based upon rocket measurements of wind and temperature together with observations from some high-level balloon soundings but since about 1971 satellite data have been used in addition. During the period 1957-72 there were also a series of rocket-grenade experiments which provided wind and temperature observations to 90km from which mean conditions up to this level could be deduced. While these experiments have been terminated, coverage to this level should soon be provided by satellites.

The early diagnostic studies showed that the lower stratosphere, between the troposphere and about 50mb at middle and high latitudes, receives energy from the troposphere. Kinetic energy is converted to potential energy in this region and the latter is dissipated by radiative processes. Above this driven region at high latitudes in winter is a region with temperature gradients similar to those in the middle latitude troposphere, with temperature decreasing polewards, where potential to kinetic energy conversion may occur. Above 10mb the energetics are not well understood and we had the following questions in mind as we commenced the present study of

the general circulation of the northern hemisphere middle stratosphere for the year 1972: What is the magnitude of the energy flux into and through the middle stratosphere? How does the energy absorbed in the middle stratosphere compare with the energy generated *in situ*? What are the physical reasons for the energy flux and for its seasonal change? Does the energy reflected by the middle and upper stratosphere have significant influence on the tropospheric circulation? The main region of interest here is that between 10 and 2mb (~30-43km) although data at lower and higher levels are included in the analysis so that the inter-relationships between levels may be studied.

## 2. DATA AND THEIR REDUCTION

The basic data used in this study are weekly and monthly grid point values of geopotential height and temperature at the 100, 10, 5 and 2mb levels for all of 1972 which were provided in the original map form by various agencies of the National Oceanic and Atmospheric Administration of the Department of Commerce, USA. Specifically, the 100 and 10mb levels, which were obtained from the National Climatic Center at Asheville, North Carolina, consisted of once-weekly 1200 Z charts for the entire year as analyzed by computer at the National Meteorological Center (NMC). The maps for the 5 and 2mb levels were obtained from the Upper Air Branch of the National Meteorological Center and consisted of: once-weekly maps for Wednesdays in January-April and September-December; maps for the middle week only for months May, June and July; and maps for the middle and last week for the month of August. It should be pointed out that the maps at the 5 and 2mb levels were hand drawn by the Upper Air Branch of NMC, based on both high-level rawinsonde and meteorological rocketsonde data at 5mb and mainly rocketsonde data at the 2mb level; some satellite data were also used in the analysis. The maps are just preliminary determinations of the wind field at those levels and represent a first effort by NMC to prepare constant-pressure charts for the upper stratosphere over the entire northern

hemisphere. Methods of chart analysis, including station coverage and correction procedures, have recently been reported in detail (Staff, Upper Air Branch NMC, 1975).

The data as received on the NMC maps (NWAC No. 555, Scale 1: 40,000,000) was reduced for use in this study as follows:

Grid values at all four levels were linearly interpolated from the maps to obtain the geopotential height (within 20 GPM) and the temperature (within 0.5°C) at every 10° latitude and longitude from 0° to 90°N. Weekly and mean monthly geostrophic wind components were then computed at 10° latitude and longitude increments from 5°N to 85°N and from 5°E to 5°W. Computation of the geostrophic wind components using finite difference approximations was as follows: (see Appendix I for definitions of notation)

$$u_{i,j} = - \frac{g}{fa} \left( \frac{H_{i+1,j} - H_{i-1,j}}{\phi_{i+1} - \phi_{i-1}} \right)$$

$$v_{i,j} = \frac{g}{fa \cos \phi_i} \left( \frac{H_{i,j+1} - H_{i,j-1}}{\lambda_{j+1} - \lambda_{j-1}} \right)$$

This allows computation of  $u$  at 5°N plus every 10° latitude to 85°N, at 0°E plus every 10° longitude. Similarly,  $v$  is computed at 5°E plus every 10° longitude to 5°W, at 0° latitude plus every 10° to 90° ( $v = 0$  at 90°N). Then by averaging the values of  $u$  at 5°N 0°E with  $u$  at 5°N 10°E and so on around the latitude circles and averaging  $v$  at 5°E 0° latitude with  $v$  at 5°E 10°N and so on along the longitude circle,  $u$  and  $v$  were computed at a common point (i.e. 5°N 5°E, 15°N 5°E, 5°N 15°E, etc.)

It is important to keep in mind the limitations in such a method of computation of wind components for a northern hemispheric cap. Due to a lack of data at low latitudes together with rather slack gradients of geopotential height there, it often proved difficult to perform a reliable computation of the wind components south of about 15°N. Where data were doubtful for 5°N or 15°N computa-

tions were omitted and the values included for these latitudes will therefore be biased and can only be used for gross comparisons.

The theoretical formulation by Eliassen and Palm (1961) was used to compute the horizontal and vertical energy flux by the large-scale planetary waves, following a precedent set by Newell (1964a), Newell and Richards (1969) and others. To find the energy flux across the four pressure levels considered, the vertical gradient of potential temperature is required at the four levels. For the 100mb level use was made of data at the 150 and 82mb levels. Temperatures at 150mb were those used in a study by Newell and Richards (1969) extended from climatological tables (Newell *et al.*, 1972). At 82mb the Oxford summaries of satellite data were used (Oxford University Department of Atmospheric Physics, 1972), again in conjunction with the climatological tables. For the 10mb level, Oxford data at 16mb and data in the present study at 5mb were used. Similarly at the 5 mb level, data from the present study at 10 and 2mb were used. Finally at 2mb (about 43km) climatological mean temperatures (and pressures) for 40 and 45km were used taken from a report by Groves (1971).

Utilizing standard statistical formulas, and the notation as outlined in Appendix I, the following quantities were computed for each pressure level:

a) At each latitude circle by week:

$[T]$ ,  $[u]$ ,  $[uv]$ ,  $[\theta]$ , horizontal energy flux, vertical energy flux and zonal harmonic analysis of geopotential for wave numbers 1 to 4.

b) At each latitude-longitude point by month:

$\bar{u}$ ,  $\bar{v}$ ,  $\bar{T}$ ,  $\bar{\theta}$ ,  $\bar{vT}$ ,  $\bar{T}^*$

c) At each latitude circle by month:

$[\bar{u}]$ ,  $[\bar{T}]$ ,  $[\bar{\theta}]$ ,  $[\bar{vT}]$ ,  $[\bar{T}]'$ ,  $[\bar{v}^*T^*]$ ,  $[\bar{v}'T']$ ,  $[\bar{v}^*T^*] + [\bar{v}'T']$ ,  $[\bar{T}^{*2}]$ ,  $[\bar{u}^{*2}]$ ,  $[\bar{v}^{*2}]$ ,  $[\bar{u}^{*2} + \bar{v}^{*2}]$ ,  $[\bar{\theta}^*\bar{v}^*]$ ,  $[\bar{u}^*\bar{v}^*]$ ,  $[\bar{u}'\bar{v}']$ ,  $[\bar{u}^*\bar{v}^* + \bar{u}'\bar{v}']$ ,  $[\bar{u}\bar{v}]$ ,  $[\sqrt{\bar{u}'^2}]$ ,  $[\sqrt{\bar{v}'^2}]$ ,  $[\sqrt{\bar{T}'^2}]$ ,  $[\bar{u}^{*2}]^{1/2}$ ,  $[\bar{v}^{*2}]^{1/2}$ ,  $[\bar{T}^{*2}]^{1/2}$ ,  $[\bar{u}'^2 + \bar{v}'^2]$ , sensible heat transfer by standing eddies, momentum transfer by standing eddies, vertical energy flux, and net radiative heating  $[\bar{Q}]$ .

- d) The following totals and area averages:  
 $\bar{T}$ ,  $\bar{\theta}$ , vertical energy flux, and  $[\bar{T}]$  by week.

Finally, the total energy contents ( $A_E$ ,  $A_Z$ ,  $K_E$ ,  $K_Z$ ), energy generation rate by radiative processes ( $G_Z$ ), and conversion rates ( $C_A$ ,  $C_K$ ) were computed for each month.

Not all the quantities listed are presented here. Many of the remainder will be tabulated in a forthcoming review.

### 3. ZONAL MEAN WIND AND TEMPERATURE FIELDS

The individual weekly maps of temperature and geopotential have been presented and discussed by the analysts at NMC (Staff, Upper Air Branch, *loc. cit.*) and it is not our intention here to reiterate this discussion although we shall make a few comments from the synoptic viewpoint later in this paper. Rather, we concentrate in this section on zonal mean values, reducing two space dimensions to one, to gain an overview of events.

Monthly values of the zonal mean west-east wind [ $u$ ] are given in Table 1 and displayed in Figure 1. In January the zonal wind is clearly westerly throughout the region except for small easterly values indicated at low latitudes at 5 and 2 mb. The polar-night jet increases with altitude to  $59 \text{ m sec}^{-1}$  at 5 mb,  $65^\circ\text{N}$  and extends downward, over a broad area, to the 100 mb level; it extends into the region just north of the upper portion of the middle latitude tropospheric jet, which appears at approximately  $35^\circ\text{N}$  at the 100 mb level with a maximum mean velocity of  $24 \text{ m sec}^{-1}$ . In February, the central velocity of the polar-night jet has decreased to  $40 \text{ m sec}^{-1}$ , although it is still positioned at approximately  $65^\circ\text{N}$ . If one follows the locus of the maximum downward it begins to move south at about 50 mb and extends into the tropospheric jet, which has increased in intensity slightly ( $26 \text{ m sec}^{-1}$ ) although still close to  $35^\circ\text{N}$ . We shall see later that the temperature increases with latitude at 2 mb and 5 mb at high latitudes consistent with this maximum.

There is a significant change in March with the upper level jet

maximum shifting southward to  $35^{\circ}\text{N}$ . Temperature now decreases with latitude in the upper layer and the maximum speed is at or above 2 mb. The locus of maximum winds extends northward with decreasing altitude, reaching  $65^{\circ}\text{N}$  at 10 mb. Concomitantly the upper portion of the tropospheric jet remains relatively stationary although somewhat decreased in magnitude ( $22 \text{ m sec}^{-1}$ ). The low-latitude easterlies have temporarily disappeared as westerlies have expanded to encompass the entire region. This change to westerlies is a manifestation of the well known semi-annual oscillation and it is more marked at the higher levels in low latitudes.

By April, the polar vortex has virtually disappeared and easterlies have replaced westerlies at high latitudes, reaching a maximum speed of  $8 \text{ m sec}^{-1}$  at 10 mb and  $65^{\circ}\text{N}$ . The westerly tropospheric jet still dominates the circulation at 100 mb, although its maximum value has decreased to  $17 \text{ m sec}^{-1}$ . By May, easterlies extend over all latitudes above 30 mb, and there are indications of the formation of a low latitude easterly jet at and above the 2 mb level probably as a result of solar heating. This easterly summer jet increases to  $35 \text{ m sec}^{-1}$  in June and  $44 \text{ m sec}^{-1}$  in July at 2 mb. The position of the maximum shifts from south of  $20^{\circ}\text{N}$  in May to  $25^{\circ}\text{N}$  in June and July. Likewise, the tropospheric jet has shifted its position northward at 100 mb and has become more broad and less intense by July, with maximum values of  $8 \text{ m sec}^{-1}$  at  $45^{\circ}\text{N}$ . August appears to be a transition month from the distinct summer regime back to the normal winter circulation with westerlies at 100 mb increasing and easterlies at 10, 5, and 2 mb decreasing. From September through December, one sees a rapid increase in the polar-night jet with the maximum velocity at 2 mb increasing from  $11 \text{ m sec}^{-1}$  in September to  $59 \text{ m sec}^{-1}$  in December. The maximum velocity was located at  $55^{\circ}\text{N}$  except in November when the polar-night jet at 2mb extended from  $25^{\circ}\text{N}$  to  $55^{\circ}\text{N}$  with values of 40 to  $44 \text{ m sec}^{-1}$  throughout the region. By December, the middle latitude tropospheric jet has shifted southward to  $35^{\circ}\text{N}$  at 100 mb and increased in velocity to  $28 \text{ m sec}^{-1}$ .

Figure 2 represents a smoothed meridional distribution of weekly

values of  $[u]$  at the 5 and 2 mb levels for 1972. Here again, the dominant westerly polar-night jet is evident at high latitudes in the winter season and the easterly jet at low latitudes in the summer months. The maximum velocity in the polar-night jet occurred in January at  $65^{\circ}\text{N}$  with speeds of  $73 \text{ m sec}^{-1}$  at 2 mb and  $67 \text{ m sec}^{-1}$  at the 5 mb level. The summer easterly jet attained maximum speeds in July at  $25^{\circ}\text{N}$  of  $44 \text{ m sec}^{-1}$  at the 2 mb level and  $28 \text{ m sec}^{-1}$  at 5 mb. Note that the westerlies change over to easterlies earlier at high latitudes than at low latitudes in the spring and the higher latitudes again precede the lower latitudes in the change back to westerlies in the fall transition. One item brought out by this presentation, not evident from the monthly means, is the evidence for weakened westerly winds at the end of February followed by a recovery in March to higher values before the change over to summer easterlies. The evidence for the semi-annual oscillation at low latitudes can also be seen with maximum westerlies at  $20^{\circ}\text{N}$  occurring at the end of March and in November.

The analysis so far has only drawn on the year 1972 and it is legitimate to question the representativeness of this year. It will be necessary to analyze several more years of observation at 5 and 2 mb before one can make judgments on this point. However, it is possible to compare the lower portion of the cross-sections here with mean monthly cross-sections for the 5 year period 1963-68 for 10-200 mb which have been presented elsewhere (Newell *et al.*, 1974a). Such a comparison shows a remarkable similarity between the 10 and 100 mb levels for 1972 and the longer term mean, the main differences occurring in the periods of change between March-April and August-October and even these differences are quite minor.

Encouraged by the similarity in the wind cross-sections and recognizing that the temperature cross-sections constructed from data at 10 and 100 mb do not give a fair picture of the complex structure between these levels, we present temperature cross-sections for 1963-68 together with the monthly values for 1972 at and above 10 mb in Figure 3. Temperature values for 100, 10, 5 and 2 mb for 1972 are presented in Table 2. Comparison between the tabulated

values for 100 and 10 mb with the cross-sections of Figure 3 shows great similarity and we deduce that 1972 was close to the climatological average in this layer. January exhibits two cold regions: one centered at the tropical tropopause and disappearing just above 50 mb, the other in polar regions centered between 30 and 50 mb but continuing up to just above 5 mb. These cold regions are separated in the lower layers by a warm region which is at  $50^{\circ}\text{N}$  at 100 mb. At 2 mb there are warm regions in the tropics and at the pole with lowest temperatures at about  $55^{\circ}\text{N}$ . In February the polar cold region is a little warmer than in January and the minimum near 30 mb has moved down in altitude. The temperature minimum at 2 mb remains at  $55^{\circ}\text{N}$ . There is a substantial difference between 1972 and 1964-68 at high latitudes near 10 mb. In March the warm-cold-warm configuration at 2 mb has given way to a decrease with latitude, yet traces of the former configuration remain at 5 mb. Polar regions have warmed and in the climatological picture at lower levels the polar cold region around 50 mb has descended further. In April there are higher temperatures than in March throughout the upper levels and at high latitudes at the lower levels. It is quite remarkable that with all these substantial changes taking place in the January-April period the temperature pattern in the vicinity of the tropical tropopause has remained essentially the same (as may be seen from a comparison of the  $200^{\circ}\text{K}$  and  $215^{\circ}\text{K}$  isotherms in January and April). Clearly, the monthly changes in the temperature structure of the winter 10-2 mb layer do not adhere to a recognizable pattern such as that indicated by Van Loon *et al.* (1975) for the 30 mb level.

A substantial change in the character of the temperature patterns occurs in May as the maximum temperatures move from tropical to polar regions. At all levels the pole is warmer than middle latitudes. Again note the invariance of the isotherms in the vicinity of the tropical tropopause. The patterns for June show a further increase which ranges from  $5^{\circ}\text{K}$  at the pole at 2 mb to  $2^{\circ}\text{K}$  in lower layers, except near the tropical tropopause. July shows evidence of still further increases at the highest levels and high latitudes, but accompanied by slight cooling at 5 and 10 mb at low latitudes. There is

cooling at all high latitudes between July and August although the maximum temperature remains over the summer pole. The reversal back to winter conditions occurs between August and September as the maximum moves to low latitudes. By October the polar cold region has reformed above 30 mb, substantially higher than the level it disappears at in the spring. Temperatures dropped by up to 15°K at the higher levels. The temperature gradients steepen during November as the pole cools further. At low levels a maximum occurs at about 55°N. Finally, in December we see again the steep gradient of January, with the cold pole, the minimum at 30 mb and moving down with time, and the almost-invariant tropical tropopause pattern.

#### 4. MEAN TEMPERATURE AND ENERGY FLUX PATTERNS

Weekly values of the zonally averaged temperature are shown in Figure 4 for latitudes between 35°N and 85°N. At the higher levels maximum values occur in the summer; there are large amplitude oscillations in the winter and spring—the latter being the well-known sudden warmings. In some of these oscillations values close to the summer maxima are attained. Previous work suggests that these oscillations are related to changes in the energy flux from the troposphere to the stratosphere (e.g., Newell, 1964a; Dopplick, 1971; Quiroz, 1975; Labitzke *et al.*, 1975) and we have therefore computed approximate values of the energy flux patterns. The formulation of Eliassen and Palm (1961) was used; it applies to large-scale, stationary, adiabatic waves and utilizes the geostrophic approximation. This gives the energy flux towards lower pressure as:

$$[pw] = [u] \frac{f [\theta^*v^*]}{\partial[\theta]/\partial z}$$

and the meridional energy flux as:

$$[pv] = -\rho[u] [u^*v^*]$$

Values of these fluxes appear in Tables 3 and 4 for the mean monthly values of the basic parameters. Weekly values of the flux towards lower pressure (henceforth termed vertical energy flux for brevity) are plotted in the lower half of Figure 4. Largest values occur at about  $65^{\circ}\text{N}$  throughout the winter months generally coinciding with the peak in the mean zonal wind: they are predominantly positive, with smaller values at the higher levels. Maximum values occur in February with minimum values close to zero during the summer easterly regime. A careful perusal of Figure 4 shows a close association between sharp temperature changes at higher levels and prior increases in energy flux from the troposphere. The main feature of the horizontal energy flux pattern, shown in Table 4, is the equatorward transport of energy away from the polar night jet region.

Mean monthly conditions were used to compute the divergence of the wave energy flux (both horizontal and vertical components) and results for selected winter months are shown in Figure 5. At lower latitudes in the lower stratosphere there is always a sink of energy (*cf.* Newell, 1964a) while at higher latitudes a source appears in the lower stratosphere in January (*cf.* Newell and Richards, 1969) that gradually changes to become a sink by March. In the middle layer there is a sink throughout the winter.

## 5. ZONAL HARMONIC ANALYSIS

A substantial amount of work has been done on the zonal harmonic analysis of the stratospheric general circulation at levels up to 10 mb: for example that by Boville (1961), Teweles (1963), Muench (1965), Hirota and Sato (1969), and Sato (1974). Similar work at higher levels has been limited by the lack of hemispheric coverage. We made a conventional zonal harmonic analysis from geopotential data at  $10^{\circ}$  longitude intervals for each  $10^{\circ}$  of latitude. Based on the findings of the earlier studies we confined the analysis to wave numbers one to four. Our best time resolution was one week between data sets in the

winter and we could not therefore effectively study the fifteen day oscillations discussed by Hirota and Sato.

Amplitude data, representing the perturbations of the geopotential field, are shown in Figure 6 for the 2mb and 5mb levels. Maximum values occur in high latitudes in winter, with very small values in the summer as might be expected from perusal of the synoptic charts which show an almost pure zonal flow from east to west. The amplitudes of wave numbers three and four are considerably smaller than those of wave numbers one and two although they follow the same general pattern with season and latitude. Wave number two has a slightly greater overall amplitude than wave number one at 5mb and 2mb, although one would have to examine several years of data to clarify this point. Comparison of Figure 6 and Figure 2 shows that both wave numbers tend to maintain their maxima at high latitudes in winter and there is a fairly close association with the zonal wind maximum, even to the extent of a small poleward displacement of both parameters early in the year and the finding that both are further south, near  $55^{\circ}\text{N}$ , at the end of December. There is also some indication that the geopotential amplitude maxima are slightly to the south of the zonal wind maxima, as predicted by Simmons (1974). Another prediction from the theory of Simmons is that maximum amplitudes of the geopotential perturbations occur in the 30-40 km layer. Figures 7 and 8 present the data in cross-section form from which the hypothesis may be tested. Figure 7 gives amplitudes based upon mean monthly data for the winter months. In January and February there were double maxima in the vertical in wave number one with a minimum at about 5 mb; wave number two showed a continuous increase with altitude. In March maximum values for both wave numbers at high latitudes occur at about 10mb. Figure 8 is a time-height section of the weekly values of amplitude at  $60^{\circ}\text{N}$ ; except in March wave number two increases in amplitude with increasing altitude while wave number one more frequently shows a maximum at 5 or 10mb. It is a challenge to the theoreticians to present an interpretation of these findings. For our part we mention three possibilities: the maxima at 5-10mb could be due to additional

reflection of wave number one, producing an enhancement there (although the theory of Charney and Drazin (1961) would predict a higher reflection coefficient for wave number two than for wave number one); the temperature perturbations associated with wave number two may lose energy by radiative dissipation at a slower rate than those of wave number one; the kinetic energy from wave number one could be selectively absorbed by the dynamical processes occurring at and above 2mb, with the subsequent conversion to potential energy and radiative dissipation. We have not subjected the various parameters involved in these ideas to harmonic analysis as would be necessary in order to make a full investigation of these possibilities.

The synoptic maps at 2 and 5mb contain the geopotential information from which these time variations of wave numbers one and two were drawn but because they represent the sum of the waves it is difficult to draw a direct association. At the beginning of January the 5mb synoptic maps show a high pressure region near the Aleutians at 50°N and another over the Atlantic at about 30°N with an extensive low pressure system centered near the pole and North Greenland with two troughs, one over the Central United States and the other from Finland to the Black Sea region. This general pattern of highs over the Pacific and Atlantic and a low in polar regions persisted throughout January at 5 mb with the two highs being joined by a third over India, then the Atlantic system and the latter amalgamating into a high over the eastern Mediterranean. The low pressure system predominated over the pole until early April when it was replaced by a high pressure system at 5mb. By May this latter system completely dominated the polar region and remained there until September, being relatively symmetric and covering much of the hemisphere during the height of the summer. Isotherms are parallel to the geopotential isopleths and the whole hemisphere is enveloped in a relatively steady easterly flow. In much of October and November the low pressure system in polar regions dominated the circulation and it was not until December that the highs regained the prominence they had in early 1972.

Large values of the vertical energy flux computed on a weekly basis, as shown from Figure 4, are associated with large values of the energy flux convergence in the 100-5mb layer. The values have been compared with the geopotential amplitude data of Figure 6; there is a general, although not a detailed, correspondence between the maxima.

The phase data from the harmonic analysis also carry significant information about the phenomena; these appear in Figure 9. It is well known that if the phase indicates a tilt of the waves westward with increasing height then an upward energy propagation is implied (*cf.* Muench, 1965). Hence in this figure if the curve at the lower level (say 5mb) lies to the right of that at the upper level (say 2mb) then an upward propagation by that component is implied. There is a clear cut difference between wave numbers one and two. In early January there is an upward propagation of energy and an eastward drift of wave number one at the 5mb and 2mb levels. Then westward propagation starts and continues until the end of March, with some further upward propagation in early March. The wave motion stands out with great clarity and passage westward round the globe occurs in about four weeks corresponding to a velocity of about  $8 \text{ msec}^{-1}$ . Some predictions of this type of wave have been made by Simmons (*loc. cit.*). At the end of March the pattern breaks down first at 5mb, then in mid-April at 2mb, and in this breakdown period the phase relationship is such that apparently a downward propagation of energy occurs. In early November the wave is again propagating westwards, changing to eastwards for December. At the 10 and 100mb levels there is little indication of this clear cut feature with a rather large oscillation in the horizontal wave propagation direction and strong evidence for upward propagation of energy.

Wave number two at 2 and 5mb also oscillates in propagation direction with the two levels fairly close in phase except in late March and April. At 10mb the phase of wave number two is fairly constant in longitude in the early part of the year, when there is an upward energy propagation.

The filtering effect produced by the lower stratosphere gives an

unusually clear portrayal of the properties of wave number one at 5mb and 2mb. The source for the excitation of this travelling wave is not known. There is a possibility that interference between the travelling wave number one and the more nearly stationary wave number two gives rise to large modulations of the energy flux. Quiroz (1975), using satellite radiance data, has suggested that the interaction of an eastward travelling wave with a standing wave in the thermal field resulted in major stratospheric warmings. The presence of a variety of travelling waves in the stratosphere has previously been reported by Deland (1973) based on satellite observations of vertically averaged temperature. He found indications, from the radiometric channel which is centered at 30mb (Channel 8, SIRS, Nimbus 3), of a westward travelling wave number one motion with a period of about one cycle per month. In our own case the clear cut wave number one is confined to high latitudes and is not evident at 40°N.

## 6. SOME ASPECTS OF THE ENERGY BUDGET

While it is not yet possible to perform a detailed study of the time evolution of the energy budget of the middle stratosphere, such as the study of daily data for the 100-10mb region by Dopplick (1971), the present data set facilitates an examination of monthly conditions for the 10-2mb region. Following the established procedures, such as those given by Dopplick (1971) as adapted from Lorenz (1955), we computed the contents of kinetic energy and available potential energy from the wind and temperature data, the conversions between the forms of energy insofar as they depend upon the quasi-horizantal motions, the generation of potential energy by radiative processes and the transfer of energy across the 10mb and 2mb pressure surfaces.

### A. ENERGY CONTENTS

We evaluate four energy contents as follows:

the zonal available potential energy

$$A_Z = C_p \int \frac{\gamma [\overline{T}]'^2}{2} dM$$

the eddy available potential energy

$$A_E = C_p \int \frac{\gamma [\overline{T^{*2}}]}{2} dM$$

the zonal kinetic energy

$$K_Z = \frac{1}{2} \int ([\overline{u}]^2 + [\overline{v}]^2) dM$$

and the eddy kinetic energy

$$K_E = \frac{1}{2} \int [\overline{u^{*2}} + \overline{v^{*2}} + \overline{u'^2} + \overline{v'^2}] dM$$

The bar in these formulations refers to time averages over a period of one month; data from one to five Wednesdays is therefore incorporated and where one only is involved deviations from the time average ( $u'$  and  $v'$ ) are obviously zero. Table 5 contains values of monthly mean temperature averaged over an isobaric surface, deviations from which are used in the computation of  $A_Z$ . The stability at 100mb and the direct influence of the sun at higher levels are evident.

Values of  $[\overline{T^{*2}}]^{1/2}$  appear in Table 6. Maximum values occur in winter at high latitudes close to the polar night jet. In the 10-2mb region there is little change with altitude, with values at 2mb a little greater than those at 5mb south of 60°N, but magnitudes are considerably larger than those at 100mb.

$K_Z$  contains mean zonal and meridional motions; the former have already been presented (Table 1) while the latter reduces to zero with our use of the geostrophic approximation. Table 7 and 8 contain values of  $[\bar{u}^*]^2]^{1/2}$  and  $[\bar{v}^*]^2]^{1/2}$ . They may be compared with values for the 100-10mb region presented in Table 8.3 and 8.4 of Newell *et al.* (1974b). The parameter  $[\bar{u}^*]^2]^{1/2}$  displays in both data sources above 100mb a double maximum in winter with a distinct minimum near 65°N close to the polar vortex mean position. At 100mb there is one maximum further south associated with the tropospheric westerly jet. Highest overall values occur in November, January and February at 5 and 2mb. The patterns of  $[\bar{v}^*]^2]^{1/2}$  again show maxima in the winter, with a single maximum associated with the polar night jet. At 10, 5, and 2mb values are considerably greater than those normal for the 1000-100mb layer; the highest values occur at 2mb although there is not a systematic increase with altitude.

Time standard deviations of  $u$  and  $v$  are presented in Tables 9 and 10. They constitute a significant contribution to the content of eddy kinetic energy. In spite of their limitation to at most five Wednesdays per month the values show good agreement with those reported by Richards (1967) for the 100 to 10mb layer which are based on all days of the month.

Energy contents computed from these parameters are shown in Table 11 for the 10-2mb layer. The first point to note is that the kinetic energy contents are greater than those of available potential energy whereas in the lower atmosphere the latter exceed the former by almost an order of magnitude. In the 10-2mb layer the motions then dominate the temperature gradients, as is obvious we inspect the large temperature changes that occur in winter in response to changes in the energy flux from below, a flux which may be regarded as an input to the kinetic energy content. The second point to note is that  $K_E$  is comparable to  $K_Z$  in winter and again this is evident from an inspection of the synoptic charts which show large asymmetries in the flow. With regard to the relative magnitudes of  $A_Z$  and  $A_E$  we note that  $A_E$  exceeds  $A_Z$  in January, February and April, the reverse being true in other months. Throughout the

summer  $A_E$  is extremely small as may have been deduced from the synoptic maps.

## B. ENERGY CONVERSIONS

The conversion between the two forms of available potential energy is given by:

$$C_A = -c_p \int \gamma [\bar{v}^* \bar{T}^* + \overline{v'T'}] \frac{1}{a} \frac{\partial [\bar{T}]}{\partial \phi} dM$$

$$-c_p \int \gamma \frac{[\bar{T}]}{[\bar{\theta}]} [\bar{\omega}^* \bar{T}^* + \overline{\omega'T'}] \frac{\partial [\bar{\theta}]}{\partial p} dM$$

Sensible heat flow down the meridional temperature gradient gives a positive contribution to  $C_A$  ( $A_Z$  to  $A_E$ ). The second term could not be computed here owing to lack of information about vertical motion for the 10 to 2mb layer. As  $\overline{v'T'}$  is based on such a small sample an alternative value for  $C_A$  with this term omitted is also shown in Table 11 and can be seen to be somewhat smaller. Both formulations show a substantial conversion from  $A_Z$  to  $A_E$  in winter, a situation similar to that in the middle latitude troposphere. Richards (1967) and Dopplick (1971) find the same sense of the conversion for the 100-10mb layer and the integrands of  $C_A$  for winter show clearly the association of the down-gradient heat transport with the polar night jet (see Newell *et al.*, 1974a).

The conversion between the two forms of kinetic energy is given by:

$$C_K = -\int [\bar{u}^* \bar{v}^* + \overline{u'v'}] \cos \phi \frac{1}{a} \frac{\partial}{\partial \phi} \frac{[\bar{u}]}{\cos \phi} dM$$

$$-\int [\bar{u}^* \bar{\omega}^* + \overline{u'\omega'}] \frac{\partial [\bar{u}]}{\partial p} dM$$

Again the second term cannot be evaluated with the present data. Negative values indicate that the Reynolds stresses are acting to build up the mean zonal flow. Evidently this is the prevailing situation in winter as may be seen from Table 11. Meridional cross-sections of the integrand of  $C_K$  have recently been presented (Newell *et al.*, 1974a) for the 200-10mb region and the association between the angular momentum transport and the mean zonal flow is clear.

There are two important conversion terms which cannot be evaluated with the present data set. The conversion between  $A_Z$  and  $K_Z$  is given by:

$$C_Z = -f[\overline{\omega}][\overline{\alpha}]' dM \cong ff[\overline{u}_g] [\overline{v}] dM$$

Physically, the conversion of  $A_Z$  to  $K_Z$  is a result of mean sinking motion in the colder latitudes and mean rising motion in the warmer latitudes. Neither  $[\overline{\omega}]$  or  $[\overline{v}]$  in the alternative formulation could be computed from the present data set. There was a similar limitation on the conversion from  $A_E$  to  $K_E$  which is given as:

$$C_E = -f[\overline{\omega}^* \overline{\alpha}^* + \overline{\omega}' \overline{\alpha}'] dM$$

### C. ENERGY GENERATION

Generation of zonal available potential energy occurs in the stratosphere when there is radiative heating at warmer latitudes and radiative cooling at colder latitudes. The approximation derived by Lorenz (1955) for this quantity is:

$$G_Z = f\gamma [\overline{Q}]' [\overline{T}]' dM$$

The radiative heating  $Q$  has three main components:

$$Q = Q_{CO_2} + Q_{O_3} + Q_{solar}$$

where  $Q_{CO_2}$  represents infrared heating by the  $15\mu m$  band of  $CO_2$ ,

$Q_{O_3}$  represents infrared heating by the  $9.6\mu\text{m}$  band of  $O_3$ , and  $Q_{\text{solar}}$  represents heating due to the absorption by ozone and ultraviolet radiation.

We were fortunate to be able to obtain up-to-date estimates of these terms from work by our colleagues. Basic information needed includes temperature cross-sections, ozone concentrations, and carbon dioxide concentration. We constructed temperature cross-sections for each month from data given in the references in Table 12. We assumed carbon dioxide had a constant volume mixing ratio of 320 parts per million. We used these two pieces of information as input to a program developed by our colleague Gerald Herman to compute the infrared heating due to  $CO_2$  for each month. We obtained ozone concentration data from our colleague Thomas Dopplack for levels below 30 km and from modelling work by Cunnold and Alyea for levels between 30 and 70km. These values correspond closely to the few measurements that have been published (see Cunnold *et al.*, 1975). The data were also used by Cunnold to compute solar heating by ozone absorption, which was supplied to us. We used the ozone concentrations, smoothed across 30km, in conjunction with the aforementioned temperature data, as input data to a computer program developed by our colleague Walter Slade to compute the infrared heating due to ozone.

Cross-sections of the three separate components of the radiative heating rate are shown in Figure 10 for January and July. For the infrared components, maximum cooling is associated with the higher temperature region near 50km. The sum of these components is shown for two mid-season months in Figure 11. Values of  $G_z$  were computed for each month for a series of layers, seven of which are listed in Table 13 so that the values for the 10-2mb layer which are included in Figure 12 may be placed in a proper perspective.

In the winter there are three characteristic regions in the energy generation: the lower stratosphere, where zonal available potential energy is destroyed by radiative processes and which we have earlier termed a refrigerated region (e.g., Newell, 1964b) by analogy with the fact that temperature gradients are maintained by an external

source of energy; the middle and upper stratosphere where energy is generated, and the mesosphere where energy is destroyed. The boundaries between regions vary even during a particular season. The mesospheric driven region occupies the layer above 0.09mb in October-January but comes down to 2mb in February and March. In the summer essentially the whole region is driven so that energy must be provided through another mechanism to maintain the radiative loss. The energy lost from the lower stratosphere is largest in summer and this probably reflects a general raising of the region of the troposphere relative to the pressure surfaces so that 197mb is closer to the tropopause and therefore the 197-76mb layer includes more of the total volume of the driven region. The tropospheric heat engine is surmounted by a refrigerator in the lower stratosphere while the winter middle stratospheric heat engine is also surmounted by a refrigerator in the lower mesosphere. The rate of energy generation in the middle stratosphere ranges up to about  $40 \times 10^{18}$  erg sec<sup>-1</sup> in October (division by two permits these numbers to be compared with those in our previous papers, *cf.* Newell, 1963, 1964a). This may be compared with the mechanical energy which is absorbed in the 10-2 mb region, as a result of forcing from below.

The details of the physical mechanisms involved are fairly clear. Warm air is cooled more than cold air in the lower stratosphere. Warm air is heated while the cold air is cooled in the middle stratosphere in winter whereas the converse occurs there in summer. A similar approach is necessary for the computation of the generation of eddy available potential energy by radiative processes. Unfortunately ozone concentrations as a function of longitude, necessary for this computation, have not yet been published for the 30-70 km region.

#### D. ENERGY TRANSFER TO AND FROM OTHER REGIONS

For the Northern Hemisphere 2-10mb layer energy may be transferred to or from the Southern Hemisphere, the region below 10mb and the region above 2mb. We have computed the convergence of the vertical energy flux in the 2-10mb layer by means of the Eliassen and Palm approximation referred to previously, this energy being an input

to  $K_E$  by the large scale quasi stationary waves. A similar input by the mean motions to  $K_Z$ , could not be computed due to lack of data on the mean meridional motion. The input to  $K_E$  is shown in Figure 12 together with the other terms that are known. Monthly values are listed in Table 14 together with fluxes and the resultant divergence between pressure levels.

#### E. ENERGY BALANCE CONSIDERATIONS

Figure 12 presents us with an overview of the energy balance on a time scale of one month. We have to bear in mind that there are four terms which are deemed significant which cannot be evaluated directly:  $G_E$ ,  $C_E$ ,  $C_Z$ , and  $[\bar{p}][\bar{w}]$ , the transfer of mechanical energy from adjacent layers into  $K_Z$ . There are in addition cross-equatorial fluxes of various forms of energy which we think are small. We can of course make rough estimates of these four terms from balance considerations with the assumption that the energy contents do not change significantly during the month. We have tacitly assumed in making balance estimates that the time changes between months are not important. To reconsider this further we note that  $A_Z$  decreases from 1.3 to 0.5 (units:  $10^{25}$  ergs) between January and February corresponding to a conversion rate of  $3 \times 10^{18}$  ergs  $\text{sec}^{-1}$ . This is fairly typical of  $A_Z$  changes with  $K_Z$  changes being somewhat larger. Let us consider the balance approach for the month of January to see where it may lead. From the balance for  $A_Z$  we deduce a value for  $C_Z$  of 42 units (one unit is  $10^{18}$  ergs  $\text{sec}^{-1}$ ). The sense is such that warm air must be sinking and cold air rising. From the temperature cross-sections it seems that much of this contribution comes from rising motion over the cold pole and sinking motion in middle latitudes. Radiative processes are insufficient to maintain the meridional temperature gradient against its reduction by the quasi-horizontal sensible heat transport and the forced mean circulation does much of the work. The energy involved can easily be supplied through the conversion  $C_K$  and hence originate from the layers below. Balance considerations for  $K_E$  then suggest that  $C_E$  is

directed towards this form again, as in the troposphere, and has a size of about 10 units. In turn we would then deduce that  $G_E$  is about 50 units and acts to reduce  $A_E$ , this being in line with events in the 30-10mb region where large amplitude waves lose energy by the process of the warmer regions cooling to space at a greater rate than the cooler regions. A similar approach applied to the February values gives  $C_Z \approx 0$  and the surplus energy supplied to  $K_Z$  via  $C_K$  must be returned to the troposphere by  $[p]''[w]''$ . More energy is supplied to  $K_E$  than appears in the transformation  $C_K$  and the difference of about 110 units must pass to  $A_E$  via  $C_E$ , a process in which warm air is forced to sink and cold air to rise. In turn warm regions cool more than cold, as for January, and  $A_E$  is reduced by  $G_E$ . The process is illustrated in Figure 13 of Newell *et al.* (1974a). The longitudinal temperature gradients at high latitudes are then largely maintained by the motions, in turn supplied with mechanical energy from below. In April-June the conversions are much smaller and there are indications that the pressure-work term associated with the mean meridional motion may be responsible for some of the energy supply. As we saw from the table of  $G_Z$  values radiative processes act to reduce the meridional temperature gradients in summer in the middle stratosphere. In September and November radiative processes act to build up the meridional temperature gradient (more cooling at high latitudes) as in the troposphere and  $A_Z$  increases. Vertical fluxes are small in this period. In November and December the flux from below increases, as does  $C_K$  and  $K_Z$ . In January and February the vertical energy flux far outweighs the generation by radiative processes.  $A_E$  exceeds  $A_Z$  in January and February presumably because the large vertical motions forced by the energy from below dominate the longitudinal temperature field; this is not the case in November and December.  $A_E$  is small throughout the summer, as is evident from the synoptic maps.

Overall we have the following picture: radiative processes create the meridional temperature gradient in the early winter; the large scale eddies convert this gradient to longitudinal gradients which are then dissipated by radiational processes; there is a steadily increasing

contribution of energy from the troposphere as the winter progresses. In February this energy supply from below swamps the energy involved in the transformations in the 10-2mb layer and at this point large temperature changes occur at high latitudes in response to the forced circulations; the warming at high latitudes shown in Figure 4 results in a large decrease in  $A_z$ .

#### F. PHYSICAL REASONS FOR CHANGES

In the above description we have said what happens but not why. The latter is difficult and elusive. One class of problems is concerned with the region just above the tropopause where a considerable amount of energy is absorbed throughout the year and radiatively lost. The energy originates in the planetary waves in the troposphere. It is absorbed in the lower stratosphere both in the summer when the winds become easterly and in the winter when they are westerly. Absorption conditions thus cannot be dependent solely upon the wind but must also depend upon vertical stability.

Energy reaches the middle stratosphere (i.e., passes through 10mb) in substantial amounts starting around November and there are large pulses in January and February. The latter occur at the time when we might expect reduced vertical transmissions as westerly winds have increased. Do these pulses originate in the troposphere or are they due to changes in conditions *in situ*? If the former is the case what are the physical mechanisms for increased upward flux? One possibility is the so-called blocking highs in the troposphere which are often associated with an above-average horizontal transport of sensible heat. Another possibility is that radiational cooling of the ground layer above a snow surface which varies spatially from week to week alters the standing wave pattern, which is impressed on the higher levels, and thereby the vertical energy flux. If events are governed by conditions at the higher levels we might speculate that higher transmission occurs when the regular motion or oscillations of wave number one bring it into a certain phase position with wave number

two, in other words an interference process occurs. We hasten to point out that we do not know the answers to these questions.

#### CONCLUDING COMMENTS

Apart from a study of the energetics of a stratospheric warming by Miller *et al.* (1972) and our previous work using a crude 6-month climatology (Newell, 1963) there has been little work on the detailed energy budget of the region above 30 km. The present study is limited to one year, which was the total length of time that hemispheric coverage was available when we performed our computations. Since then data for a further six months has become available. The variability at these upper levels seems quite large particularly in winter and data for several more years must be analyzed before we can claim to have established the climatology and the mean energy budget.

At this stage it should perhaps be stressed that once-weekly maps are not sufficient to catch the active propagating waves that appear to be present. A three day time resolution is desirable.

It is also imperative to obtain longitudinal coverage of ozone concentration at these upper levels in order to obtain correct radiative heating rates. (This same comment was made in our 1963 paper on the same topic.)

We stress the problem which apparently exists in reconciling the energy budget of the middle stratosphere in summer: radiative processes destroy zonal available potential energy. Is there an unknown energy source or are there cumulative errors in the radiation computations?

Finally we have argued elsewhere (Newell, 1964a) that total ozone is a sensitive indicator of the vertical flux of energy through the lower stratosphere. If this is correct we have an additional reason for aiming to understand the details of the stratosphere energy budget.

## APPENDIX I

## NOTATIONS AND DEFINITIONS

$C_p$  = specific heat at constant pressure =  $1.0046 \times 10^7 \text{ erg gm}^{-1} \text{ }^\circ\text{K}^{-1}$

$R$  = gas constant for dry air =  $2.8704 \times 10^6 \text{ erg gm}^{-1} \text{ }^\circ\text{K}^{-1}$

$T$  = temperature in degrees Kelvin

$\theta$  = potential temperature in degrees Kelvin =  $T \left( \frac{P_{00}}{p} \right)^k$

$t$  = time

$P_{00}$  = 1 000mb

$p$  = pressure

$K = \frac{R}{C_p} = 0.286$  for dry air

$a$  = radius of the earth =  $6.371 \times 10^8 \text{ cm}$

$g$  = gravitational acceleration =  $9.8062 \times 10^2 \text{ cm sec}^{-2}$

$\phi$  = latitude, measured northward

$\lambda$  = longitude, measured eastward

$\Omega$  = earth's angular velocity =  $7.292 \times 10^{-5} \text{ sec}^{-1}$

$f$  = Coriolis parameter =  $2 \Omega \sin \phi$ .

$H$  = geopotential height

$u$  = west wind component (positive if from west) =  $-\frac{g}{fa} \frac{\partial H}{\partial \phi}$

$v$  = south wind component (positive if from south) =  $g (fa \cos \phi)^{-1} \frac{\partial H}{\partial \lambda}$

$\omega$  = vertical velocity in pressure coordinates =  $\frac{dp}{dt}$

$w$  = vertical velocity in height coordinates =  $\frac{dz}{dt}$

$\rho$  = density

$\alpha$  = specific volume

$Q$  = rate of non-adiabatic heating per unit mass

$$dM = \text{increment of mass} = \rho dx dy dz = a^2 \cos \phi d\phi d\lambda \left( - \frac{dp}{g} \right)$$

$$\gamma = \left( \bar{\bar{T}} - \frac{p C_p}{R} \frac{\partial \bar{\bar{T}}}{\partial p} \right)^{-1} = \text{stability parameter}$$

$x$  = arbitrary dependent variable

$\bar{x}$  = time average of  $x$

$x'$  = deviation from time average

$[x]$  = zonal average of  $x$

$x^*$  = deviation from zonal average

$[x]''$  = deviation from meridional average



5 mb

Lat.	Jan.	Feb.	Mar.	Apr.	May	June	July	Aug.	Sept.	Oct.	Nov.	Dec.
85	14.5	12.8	0.8	0.9	2.9	4.1	4.0	0.9	1.3	6.2	6.2	8.8
75	43.1	34.8	10.5	5.5	6.5	8.2	14.5	3.4	6.9	19.1	17.6	31.6
65	59.0	39.9	19.3	7.2	9.2	9.6	15.0	4.8	7.5	23.1	26.5	41.9
55	50.9	29.7	17.5	3.7	10.4	12.4	16.5	8.5	8.5	21.7	29.5	43.8
45	31.6	15.2	14.6	3.0	10.8	14.7	18.4	11.5	5.9	18.4	27.9	34.8
35	13.0	7.9	18.2	8.1	7.9	16.7	23.2	15.2	1.8	11.0	25.8	25.5
25	2.2	8.7	8.5	3.9	6.4	23.2	27.7	16.6	6.8	6.8	23.0	16.9
15	3.6	3.0	0.4	3.8	7.5	8.7	23.2	14.1	6.6	5.1	17.3	11.8

2 mb

85	17.7	12.8	0.8	0.8	1.3	1.6	2.0	2.3	1.8	8.0	3.5	9.4
75	43.7	27.5	8.0	1.7	5.2	2.5	10.4	4.8	8.5	24.8	20.1	33.7
65	57.8	31.8	15.7	1.0	9.1	12.3	15.3	10.0	11.4	28.8	35.2	50.5
55	52.3	27.6	21.5	1.9	10.3	17.6	20.5	12.3	11.1	30.9	41.1	59.3
45	42.4	24.4	28.6	5.5	9.7	20.7	26.6	15.4	9.1	29.1	43.7	54.7
35	27.8	18.2	29.7	7.0	11.6	28.2	31.7	19.8	5.4	25.6	44.0	50.2
25	14.3	14.3	17.7	5.3	16.6	35.0	44.2	11.3	0.9	24.6	40.7	30.2
15	2.2	4.7	6.7	3.2	29.5	29.1	24.1	7.3	7.1	21.8	29.9	18.0

TABLE 1 - Continued

Lat.	100 mb											
	Jan.	Feb.	Mar.	Apr.	May	June	July	Aug.	Sept.	Oct.	Nov.	Dec.
85	209.2	206.5	213.0	227.5	226.9	229.2	230.5	228.8	224.2	220.5	215.0	205.9
75	210.6	209.1	214.4	225.8	226.0	228.1	228.8	227.4	223.8	220.8	216.5	208.8
65	213.9	213.2	217.1	223.0	224.1	225.5	225.6	224.8	222.5	219.9	217.8	213.2
55	217.4	217.0	218.4	219.2	220.6	221.5	221.2	220.6	219.5	217.6	217.0	216.2
45	216.5	216.7	216.5	214.8	216.0	215.6	214.6	213.9	214.1	213.5	213.6	215.1
35	210.7	210.2	210.4	209.2	209.8	208.0	207.0	206.2	206.8	207.2	207.2	209.4
25	203.7	201.7	202.5	202.5	202.5	201.7	201.3	200.8	200.6	200.8	200.0	202.3
15	199.2	197.3	197.8	198.1	197.7	198.6	197.9	197.7	197.2	196.3	195.5	197.4
5	197.7	196.2	196.3	196.5	196.3	197.5	196.3	196.2	195.8	193.7	193.4	195.1

Lat.	10 mb											
	Jan.	Feb.	Mar.	Apr.	May	June	July	Aug.	Sept.	Oct.	Nov.	Dec.
85	203.6	213.8	227.2	232.5	237.1	242.1	244.2	238.7	227.3	214.2	208.3	203.3
75	208.2	216.7	227.5	231.7	236.9	241.4	243.4	238.3	228.4	216.2	210.2	206.5
65	214.2	220.5	227.0	230.3	236.2	239.8	241.3	237.4	230.0	219.6	213.5	211.5
55	220.1	223.6	226.2	229.2	235.1	237.3	238.6	236.0	231.0	223.5	217.6	216.8
45	225.5	226.8	226.8	229.6	234.3	234.8	236.4	234.5	231.6	226.7	222.2	221.5
35	229.3	229.5	228.7	231.5	234.2	233.3	234.5	233.0	231.9	228.9	226.3	225.6
25	231.1	230.7	230.4	233.6	234.7	232.9	233.3	231.8	231.7	230.0	228.9	228.6
15	231.9	231.4	231.4	234.7	235.2	232.9	232.3	231.0	231.3	230.7	230.2	230.0
5	232.1	232.0	231.9	235.2	235.5	233.1	231.3	230.5	230.8	231.2	231.0	230.8

TABLE 2. Zonal Average of Mean Monthly Temperature,  $[\bar{T}]$ , 1972. Units:  $^{\circ}\text{K}$ .

5 mb

Lat.	Jan.	Feb.	Mar.	Apr.	May	June	July	Aug.	Sept.	Oct.	Nov.	Dec.
85	221.7	245.5	236.1	241.0	250.6	255.0	259.8	254.4	237.7	222.5	214.7	211.9
75	223.8	241.3	233.9	241.6	249.8	254.5	258.5	252.9	238.5	224.3	216.3	213.3
65	227.7	237.0	232.4	242.9	249.6	253.7	256.3	250.3	239.7	227.5	219.8	216.8
55	232.4	235.8	233.9	244.6	249.6	252.4	253.5	247.5	240.9	231.3	224.9	223.2
45	236.2	236.8	237.8	246.1	249.2	250.7	250.5	245.2	242.1	235.3	230.7	231.9
35	239.1	238.8	242.0	247.1	248.1	248.8	247.2	243.6	243.6	239.0	236.5	239.7
25	241.4	240.9	244.7	247.5	246.5	247.1	244.2	243.1	245.1	242.9	241.6	243.7
15	242.7	242.5	245.5	247.6	245.0	245.8	242.1	243.5	246.0	246.2	245.3	244.8
5	243.0	243.2	245.7	247.6	243.8	245.1	241.0	244.4	246.7	248.2	247.1	244.8

2 mb

85	251.1	256.0	246.3	254.6	271.9	277.2	279.7	270.6	250.4	231.0	226.9	227.3
75	249.7	254.3	246.4	256.5	271.3	276.7	279.2	269.8	251.9	234.5	228.0	228.5
65	247.0	251.2	247.6	260.0	270.4	274.3	278.0	267.7	254.0	240.0	231.0	231.7
55	245.6	249.0	251.0	263.2	269.2	271.1	276.1	265.0	255.8	245.6	236.8	238.2
45	248.8	251.5	256.8	265.4	268.2	268.8	273.4	262.9	257.4	251.2	245.0	247.1
35	254.7	257.1	262.7	266.5	267.3	266.6	270.0	261.6	259.2	256.6	252.9	255.7
25	259.6	261.0	266.6	266.6	266.5	264.4	266.3	261.0	260.7	260.7	258.5	260.8
15	261.9	262.3	268.3	266.5	265.2	262.8	263.1	261.1	261.8	263.3	261.9	262.2
5	262.2	262.5	269.1	266.5	264.0	261.5	261.9	261.4	262.4	264.8	263.8	262.4

TABLE 2 - Continued.

Lat.	100 mb											
	Jan.	Feb.	Mar.	Apr.	May	June	July	Aug.	Sept.	Oct.	Nov.	Dec.
85	0.0	0.0	0.0	0.0	0.0	0.0	0.0	0.0	0.0	0.0	0.0	0.0
75	-172.5	586.8	31.1	59.2	0.4	0.0	-12.6	6.2	3.1	-	8.6	-195.9
65	-210.3	667.4	115.1	51.8	5.9	0.2	-5.6	-8.0	9.4	-	36.7	-16.9
55	-205.4	-19.0	216.0	0.7	9.4	-0.9	-11.5	-11.2	14.1	-	150.2	-249.9
45	-473.1	-320.9	-1.5	27.0	38.0	11.7	-28.0	35.4	-17.3	-	241.7	-438.7
35	-556.4	-610.8	-106.3	-86.5	-0.4	-7.4	-44.1	-48.8	-148.1	-	47.2	-389.2
25	-64.8	-40.5	-81.6	-32.2	-80.3	-13.9	7.2	41.0	-49.4	-	105.7	-172.8
15	-27.1	51.6	-30.2	126.3	-5.0	24.2	-27.3	0.0	1.7	-	94.3	-115.0

Lat.	10 mb											
	Jan.	Feb.	Mar.	Apr.	May	June	July	Aug.	Sept.	Oct.	Nov.	Dec.
85	0.0	0.0	0.0	0.0	0.0	0.0	0.0	0.0	0.0	0.0	0.0	0.0
75	-97.0	-32.2	-53.3	5.7	0.5	0.1	0.0	0.1	-1.1	5.9	-64.8	-69.6
65	-163.3	-195.9	-86.3	7.8	-0.6	-0.2	0.8	0.5	-2.4	-12.7	-152.2	-180.4
55	-303.1	-300.6	-95.9	10.1	-0.4	2.5	0.2	0.9	-1.6	-20.2	-135.4	-188.9
45	-90.8	-116.3	-29.0	-0.6	-0.1	1.4	-0.2	0.1	0.1	-14.3	-47.4	-54.7
35	-5.5	-24.4	-9.5	-3.9	0.3	2.5	-1.4	-3.7	0.3	0.1	-7.2	-16.2
25	4.9	4.3	1.1	-0.4	1.0	-0.2	-10.9	-14.2	-1.0	0.4	0.8	0.6
15	-3.8	2.6	0.9	-0.5	0.8	-2.3	-8.4	-17.9	-1.4	-1.5	0.5	-0.4

TABLE 4. Horizontal Energy Flux, [pV]. Units:  $10^2$  ergs  $\text{cm}^{-2}$   $\text{sec}^{-1}$ .  
(NOTE: 0.0 represents  $\leq \pm 0.05 \times 10^2$ )

5 mb

Lat.	Jan.	Feb.	Mar.	Apr.	May	June	July	Aug.	Sept.	Oct.	Nov.	Dec.
85	0.0	0.0	0.0	0.0	0.0	0.0	0.0	0.0	0.0	0.0	0.0	0.0
75	20.6	187.5	- 11.3	1.7	2.6	1.0	3.0	0.6	0.2	4.3	- 96.5	- 88.8
65	- 315.4	88.6	- 100.7	0.9	- 1.5	0.7	1.7	- 0.4	0.2	2.5	- 161.0	- 220.6
55	- 215.7	- 58.4	- 70.2	0.0	- 1.9	0.3	2.0	- 0.7	- 0.1	- 10.8	- 110.2	- 169.9
45	- 45.1	- 25.2	- 30.2	0.3	- 2.2	0.3	1.0	- 0.4	0.8	1.9	- 11.4	- 87.1
35	- 23.5	- 9.6	- 27.6	- 0.8	0.6	0.3	7.7	0.4	0.0	1.8	- 3.7	- 27.9
25	- 1.1	- 3.1	- 5.5	1.5	- 0.3	0.2	10.6	- 0.7	- 0.6	0.6	- 0.3	- 3.8
15	4.2	0.1	- 0.5	1.7	- 0.2	- 0.4	55.3	- 4.8	0.0	- 0.5	1.9	- 19.6

2 mb

85	0.0	0.0	0.0	0.0	0.0	0.0	0.0	0.0	0.0	0.0	0.0	0.0
75	1.6	25.1	- 0.9	0.2	0.4	0.0	0.3	- 0.2	0.0	- 8.5	- 62.6	- 33.5
65	- 216.9	- 7.1	- 9.5	0.0	- 1.6	0.1	0.1	- 2.0	0.3	- 7.7	- 145.0	- 74.4
55	- 199.5	- 53.7	- 17.8	- 0.1	- 0.2	0.3	0.1	- 0.5	- 0.6	- 5.0	- 101.5	- 126.4
45	- 115.0	- 39.8	- 14.7	0.0	- 1.0	0.4	0.8	1.4	- 0.2	0.8	- 28.3	- 94.2
35	- 45.6	- 20.9	- 17.6	- 0.3	0.0	- 0.3	- 1.3	1.1	0.0	- 0.6	- 9.7	- 40.6
25	- 11.0	- 1.0	0.9	0.1	- 3.1	- 7.1	- 2.3	- 0.3	0.0	- 1.7	- 6.0	- 6.4
15	0.1	0.0	- 7.1	- 0.3	- 1.6	- 11.4	0.7	- 0.3	0.8	- 0.3	- 19.4	- 11.3

TABLE 4 - Continued

Lat.	100 mb											
	Jan.	Feb.	Mar.	Apr.	May	June	July	Aug.	Sept.	Oct.	Nov.	Dec.
85	- 1.9	- 11.0	- 1.4	- 1.2	0.0	- 0.2	0.8	0.2	- 0.1	- 0.3	- 0.8	9.4
75	15.1	33.3	13.1	25.6	0.2	0.0	4.9	4.1	1.4	11.5	4.6	208.3
65	214.9	642.2	326.3	94.5	4.3	0.3	1.9	3.1	16.4	86.8	268.6	327.6
55	459.6	774.0	365.0	91.4	7.8	1.4	4.1	7.0	40.4	127.7	469.8	295.2
45	167.1	352.9	105.5	51.4	- 4.5	- 3.8	16.1	4.3	34.9	54.0	196.1	165.8
35	- 56.4	- 5.7	42.1	7.9	- 14.9	6.9	2.0	- 0.6	0.2	11.1	- 42.1	- 14.3
25	- 28.1	- 41.7	16.4	- 4.3	- 1.6	2.9	- 8.0	- 1.7	0.7	- 4.0	- 32.0	- 65.2
15	- 1.9	- 6.3	8.4	- 3.7	4.2	- 6.3	- 7.4	- 2.3	- 0.2	0.6	- 5.5	- 19.4
	10 mb											
85	15.5	34.1	5.4	0.2	- 0.1	- 0.1	0.0	0.0	0.0	0.1	5.1	2.7
75	273.5	416.7	65.6	2.4	- 1.2	- 1.1	- 0.3	- 0.3	0.9	5.6	85.1	61.7
65	384.4	530.7	76.2	0.9	- 2.2	- 2.3	- 0.3	- 0.9	1.7	19.4	127.6	149.4
55	176.8	244.8	33.4	- 2.6	- 1.2	- 3.0	- 0.9	- 1.1	0.8	15.1	78.4	125.2
45	39.9	42.2	7.8	0.2	- 0.1	- 1.8	- 0.6	- 0.8	0.1	3.2	18.8	44.3
35	3.6	2.8	0.8	- 0.5	0.0	- 0.5	0.2	- 1.2	0.0	0.2	2.0	9.3
25	0.2	0.2	0.0	- 0.1	0.2	- 0.1	- 0.7	- 0.8	- 0.2	0.0	0.1	0.9
15	0.0	0.0	0.0	0.0	0.1	- 0.3	- 0.6	- 0.3	0.0	- 0.2	0.0	0.0

TABLE 3. Vertical Energy Flux, [ $\text{pW}$ ]. Units:  $\text{ergs cm}^{-2} \text{sec}^{-1}$ .

5 mb

Lat.	Jan.	Feb.	Mar.	Apr.	May	June	July	Aug.	Sept.	Oct.	Nov.	Dec.
85	3.2	10.2	0.2	0.0	- 0.1	0.0	0.0	0.0	0.0	0.0	2.1	1.0
75	76.9	160.5	12.8	1.3	- 0.9	- 0.1	0.1	0.3	- 0.1	0.8	32.0	27.1
65	173.4	231.7	30.6	1.8	- 0.4	- 0.1	0.1	0.2	- 0.1	2.6	49.7	59.9
55	113.6	113.7	17.9	0.4	0.0	- 0.1	0.5	0.0	- 0.2	2.2	29.7	37.7
45	32.6	21.2	6.7	0.0	0.0	0.0	0.5	- 0.2	0.0	1.2	7.9	9.8
35	3.9	2.0	2.6	0.0	0.0	0.0	0.3	- 0.3	0.0	0.5	0.5	1.8
25	0.1	0.1	0.4	0.0	0.0	0.0	0.2	0.0	0.0	0.0	0.1	0.4
15	0.0	0.0	0.0	0.0	0.0	0.0	0.0	0.0	0.0	0.1	0.0	0.2

2 mb

85	0.9	10.0	0.1	0.0	0.0	0.0	0.0	0.0	0.0	0.1	1.6	0.2
75	39.7	110.2	5.4	0.1	- 0.2	0.0	0.5	0.2	- 0.1	0.9	42.4	12.3
65	158.2	141.2	12.8	0.0	- 0.5	0.0	1.0	1.0	- 0.2	1.1	68.6	42.6
55	151.4	86.3	10.8	0.0	- 0.2	- 0.2	1.2	0.5	- 0.2	0.4	39.5	45.2
45	46.9	34.7	7.3	0.2	0.0	- 0.2	0.2	0.4	0.0	- 0.7	7.6	17.5
35	6.1	7.2	2.3	0.2	- 0.3	0.5	0.8	0.2	0.0	0.6	0.1	3.3
25	0.4	0.9	0.4	0.0	- 0.4	1.1	0.6	- 0.1	0.0	0.3	0.1	0.4
15	0.0	0.0	0.0	0.0	- 0.2	0.4	0.1	- 0.1	0.1	0.1	- 0.6	- 0.1

TABLE 3. Continued

<i>Month</i>	<i>100 mb</i>	<i>10 mb</i>	<i>5 mb</i>	<i>2 mb</i>
Jan.	207.3	226.9	238.2	255.8
Feb.	206.1	228.3	240.4	257.8
Mar.	207.1	229.6	241.5	261.7
Apr.	208.1	232.8	246.6	265.3
May	208.4	235.4	247.4	267.4
June	208.7	235.0	249.0	267.0
July	208.0	235.4	247.5	269.4
Aug.	207.5	233.5	245.6	263.2
Sept.	206.9	231.4	244.0	259.3
Oct.	205.8	227.8	239.7	255.7
Nov.	205.0	225.1	236.6	251.8
Dec.	205.6	224.4	236.5	252.9

TABLE 5. Mean Temperature Averaged Over an Isobaric Surface,  $\bar{T}$ . Units: °K.





100 mb												
Lat.	Jan.	Feb.	Mar.	Apr.	May	June	July	Aug.	Sept.	Oct.	Nov.	Dec.
85	7.8	6.2	5.9	5.6	1.4	3.2	1.9	1.6	2.2	2.1	2.0	5.3
75	7.3	8.5	5.8	2.7	1.5	1.6	2.3	2.4	2.4	2.6	5.7	6.1
65	5.9	5.5	2.6	2.8	1.8	2.1	1.8	1.3	1.7	3.2	3.1	3.2
55	7.5	7.1	7.0	3.4	3.0	3.1	2.8	2.8	3.7	4.1	4.7	7.4
45	9.4	11.0	6.6	5.3	3.4	4.3	5.7	5.7	4.5	7.7	6.1	8.9
35	8.6	8.8	6.2	5.6	3.9	5.7	5.5	4.6	6.3	8.0	11.2	9.5
25	6.2	5.7	4.6	3.7	3.9	4.5	8.2	6.4	5.7	7.6	5.4	5.6
15	6.0	4.9	5.1	5.4	7.5	11.7	9.2	6.6	6.7	6.2	4.6	6.7
10 mb												
85	14.4	19.7	15.1	2.6	1.2	0.7	0.6	1.3	1.4	4.0	18.2	6.9
75	19.5	15.9	9.9	4.2	1.0	1.0	1.1	0.9	1.8	3.6	10.7	7.4
65	4.7	6.8	6.4	2.6	0.7	1.3	1.2	1.1	1.7	3.7	4.3	5.8
55	16.2	13.6	9.8	4.5	1.1	1.3	0.8	1.1	2.1	5.0	13.7	6.3
45	18.3	17.8	10.7	4.8	1.9	1.8	1.8	1.9	2.0	5.4	13.9	8.8
35	13.6	14.0	7.3	4.0	1.5	3.3	3.4	3.1	2.0	4.3	8.5	10.1
25	7.7	8.1	4.7	4.0	2.5	2.5	3.4	4.9	3.8	5.0	3.8	7.1
15	4.1	3.4	3.0	3.3	2.9	4.4	6.7	4.2	3.2	3.6	2.1	2.2

TABLE 7. Spatial Standard Deviations of  $\bar{u}$ ,  $\sqrt{[\bar{u}^2]}$ . Units: m sec<sup>-1</sup>.



Lat.	100 mb											
	Jan.	Feb.	Mar.	Apr.	May	June	July	Aug.	Sept.	Oct.	Nov.	Dec.
85	5.6	6.0	4.8	3.2	1.4	2.2	1.6	1.4	1.8	2.3	2.2	5.2
75	11.6	13.2	10.2	5.3	2.9	4.0	2.6	2.9	3.3	4.4	4.4	10.9
65	12.0	14.7	9.8	3.9	2.8	3.2	3.1	3.4	3.2	5.2	5.5	10.6
55	9.2	12.0	6.6	3.7	3.0	3.1	3.7	3.5	3.0	5.2	5.5	8.1
45	5.6	6.7	4.2	3.9	3.3	3.0	4.4	3.7	3.4	5.0	5.4	5.5
35	3.8	3.8	3.6	3.4	3.4	3.3	4.4	3.3	3.5	5.3	4.9	4.6
25	3.3	3.6	3.7	4.1	3.8	4.7	4.2	3.1	3.9	4.4	4.3	4.9
15	3.5	3.2	3.3	4.7	4.2	4.9	3.6	3.2	3.7	6.2	4.7	4.7
	10 mb											
85	9.8	12.0	9.4	1.8	1.2	0.6	0.7	1.1	1.4	2.8	9.5	4.1
75	23.0	25.0	18.6	3.4	2.1	1.3	1.2	1.9	2.6	5.8	17.6	8.9
65	24.5	24.6	16.7	3.9	1.9	1.8	1.3	1.7	2.7	6.2	14.1	9.6
55	16.8	18.9	11.8	3.3	1.6	1.8	1.5	1.4	2.0	5.0	9.2	8.4
45	8.6	11.4	6.9	3.2	1.7	2.0	2.3	1.7	1.6	3.0	4.8	6.0
35	4.8	5.5	3.8	3.3	2.6	2.4	3.4	2.8	2.2	2.0	2.5	3.7
25	3.4	3.0	2.5	3.0	2.9	3.3	4.3	4.2	2.3	2.0	1.6	2.0
15	4.0	2.8	2.5	3.7	2.9	3.2	5.0	5.9	2.6	3.3	1.8	1.6

TABLE 8. Spatial Standard Deviations of  $\bar{v}$ ,  $\sqrt{[\bar{v}^2]}$ . Units: m sec<sup>-1</sup>.







Lat.	100 mb											
	Jan.	Feb.	Mar.	Apr.	May	June	July	Aug.	Sept.	Oct.	Nov.	Dec.
85	4.4	3.4	4.4	2.4	1.9	1.6	2.3	1.8	2.9	2.5	3.2	4.4
75	7.7	7.3	9.2	4.1	3.2	2.5	3.6	3.5	4.3	4.7	5.5	7.0
65	6.9	7.5	9.7	4.3	3.6	2.4	3.7	4.7	4.3	6.1	5.9	7.0
55	5.9	5.7	7.5	5.0	4.3	3.2	4.5	5.6	4.9	6.3	6.2	8.2
45	5.2	4.4	5.3	4.9	4.3	3.7	4.8	5.6	4.2	6.6	6.7	8.1
35	4.9	5.1	5.9	5.5	3.9	3.2	4.1	4.4	4.0	6.2	6.3	6.8
25	4.8	4.6	5.4	5.5	4.0	3.9	3.6	3.9	3.7	5.6	5.3	6.2
15	4.2	3.7	4.2	4.7	4.2	4.7	3.9	3.9	2.9	5.8	4.4	4.9
	10 mb											
85	6.4	9.8	7.6	2.0	1.6	0.7	0.9	1.5	1.7	2.8	4.6	2.9
75	14.9	21.2	14.2	3.9	2.1	1.4	1.7	2.3	2.7	5.0	8.2	6.0
65	17.5	23.0	12.2	4.7	1.5	1.7	1.9	2.0	2.5	5.1	7.8	7.1
55	14.8	18.3	8.4	4.5	1.6	1.7	1.8	1.8	2.4	4.6	6.6	7.0
45	9.5	10.9	4.7	3.8	1.8	2.1	2.1	2.0	2.2	3.4	5.0	5.4
35	5.2	5.5	2.9	3.6	1.9	2.1	3.0	2.3	2.5	2.5	3.0	3.2
25	2.9	2.9	2.3	4.0	2.1	2.9	3.9	3.2	2.6	2.3	2.2	1.6
15	2.7	2.5	2.9	4.6	2.3	3.4	4.0	4.9	3.3	3.1	2.7	1.6

TABLE 10. Zonally Averaged Time Standard Deviations of  $v$ ,  $[\sqrt{v^2}]$ . Units: m sec<sup>-1</sup>.



Month	ALT				ALT			
	A <sub>Z</sub>	A <sub>E</sub>	K <sub>E</sub>	K <sub>Z</sub>	C <sub>A</sub>	C <sub>A</sub>	C <sub>K</sub>	C <sub>K</sub>
Jan.	1.3	1.7	7.7	7.9	58.7	33.6	-82.9	-80.1
Feb.	0.5	1.1	6.8	3.4	6.7	0.1	-41.4	-28.2
Mar.	0.8	0.4	3.2	1.9	10.4	7.2	-24.7	-19.7
Apr.	0.1	0.3	1.1	0.4	-0.3	-0.3	1.6	0.04
May	0.1	0.02	0.5	1.7	-0.1	-0.1	2.5	2.5
June	0.3	0.1	0.8	3.0	-0.1	-0.06	0.7	0.7
July	0.7	0.1	0.7	4.9	-0.4	-0.4	-0.6	-0.6
Aug.	0.2	0.03	0.5	1.9	0.2	0.03	-0.5	0.14
Sept.	0.2	0.04	1.0	0.4	0.3	-0.1	-0.7	0.3
Oct.	1.5	0.1	1.0	2.6	3.6	1.8	0.6	-0.9
Nov.	2.8	0.4	3.2	5.7	32.0	23.3	-13.9	-12.6
Dec.	3.2	0.6	3.6	7.6	26.9	24.8	-65.0	-42.1

TABLE 11. Total Energy Contents for the 10-2 mb layer - A<sub>Z</sub>, A<sub>E</sub>, K<sub>Z</sub> and K<sub>E</sub>  
(Units: 10<sup>25</sup> ergs) and Conversion Rates - C<sub>A</sub>, ALT C<sub>A</sub>, C<sub>K</sub> and ALT C<sub>K</sub> (Units: 10<sup>18</sup> ergs sec<sup>-1</sup>).

TABLE 12. Data Sources for Radiative Heating Rate Computations

Parameter	Region (km)	Source of data or calculation technique
T	0–22	Oort and Rasmusson (1971) and Crutcher and Meserve (1970)
T	22–44	Tahnk (1973)
T	44–70	Theon, Smith, Casey and Kirkwood (1972)
O <sub>3</sub>	0–30	Dopplick (private communication)
O <sub>3</sub>	30–70	Cunnold (private communication)
CO <sub>2</sub>	0–70	Herman (1972)
Q <sub>O<sub>3</sub></sub>	0–70	Slade (1975)
Q <sub>CO<sub>2</sub></sub>	0–70	Herman (1972)
Q <sub>solar</sub>	0–70	Cunnold (private communication)

Table 13. Generation of Zonal Available Potential Energy in Pressure Layers.

p(mb)	Units: $10^{18}$ ergs $\text{sec}^{-1}$									
	197-26	26-11.6	10-5	5-2	2-1	1-0.09	0.09-0.04			
January	- 176	- 0.6	2.6	5.2	4.6	1.9	- 0.12			
February	- 167	0.5	2.6	3.8	3.0	- 1.1	- 0.27			
March	- 170	- 0.6	2.3	2.5	0.1	- 1.2	- 0.30			
April	- 232	- 1.3	- 0.3	0.1	- 0.1	- 0.6	- 0.13			
May	- 289	- 1.6	0	0.5	0	0.3	- 0.19			
June	- 326	- 8.4	- 0.5	- 1.8	- 1.1	0.7	- 0.04			
July	- 360	- 15.3	- 4.9	- 5.8	- 3.4	- 1.5	- 0.12			
August	- 284	- 14.4	- 3.4	- 3.0	- 2.4	- 3.1	- 0.03			
September	- 242	- 6.5	1.0	2.3	1.2	- 0.5	- 0.09			
October	- 232	- 0.3	3.1	5.7	3.4	1.1	- 0.38			
November	- 245	1.7	0.2	5.4	5.5	3.0	- 0.04			
December	- 204	1.8	0.1	4.3	5.5	2.7	- 0.26			

Month	100 mb	10 mb	5 mb	2 mb	100-10	10-5	5-2	10-2
Jan.	179.4	163.2	82.3	90.2	- 16.2	- 80.9	7.9	- 73.0
Feb.	403.6	225.4	98.7	75.8	- 178.2	- 126.7	- 22.9	- 149.6
Mar.	215.1	33.2	15.0	9.1	- 181.9	- 18.2	- 5.9	- 24.1
Apr.	59.6	- 0.4	0.6	0.2	- 60.0	1.0	- 0.4	0.6
May	- 2.8	- 0.8	- 0.1	- 0.5	2.0	0.7	- 0.4	0.3
June	- 0.2	- 2.3	- 0.1	0.7	- 2.1	2.2	0.8	3.0
July	1.1	- 1.0	- 0.5	0.2	- 2.1	0.5	0.7	1.2
Aug.	2.2	- 1.6	- 0.1	0.5	- 3.8	1.5	0.6	- 2.1
Sept.	24.8	0.6	- 0.04	0.1	- 24.2	- 0.6	0.1	- 0.5
Oct.	69.7	9.1	1.7	0.1	- 60.6	- 7.4	- 1.6	- 9.0
Nov.	207.2	60.6	23.3	30.1	- 146.6	- 37.3	6.8	- 30.5
Dec.	173.0	85.0	27.9	27.8	- 88.0	- 57.1	- 0.1	- 57.2

TABLE 14. Total Vertical Energy Flux (Units:  $10^{18}$  ergs  $\text{sec}^{-1}$ ) and Resultant Divergence Between Levels (positive sign indicates divergence).

## ACKNOWLEDGMENTS

This work was supported by the United States Energy Research and Development Administration under Contract No. AT(11-1)-2195. We are very grateful to our colleagues Derrick Cunnold, Gerald Herman and Walter Slade for their help in providing radiative heating rate computations.

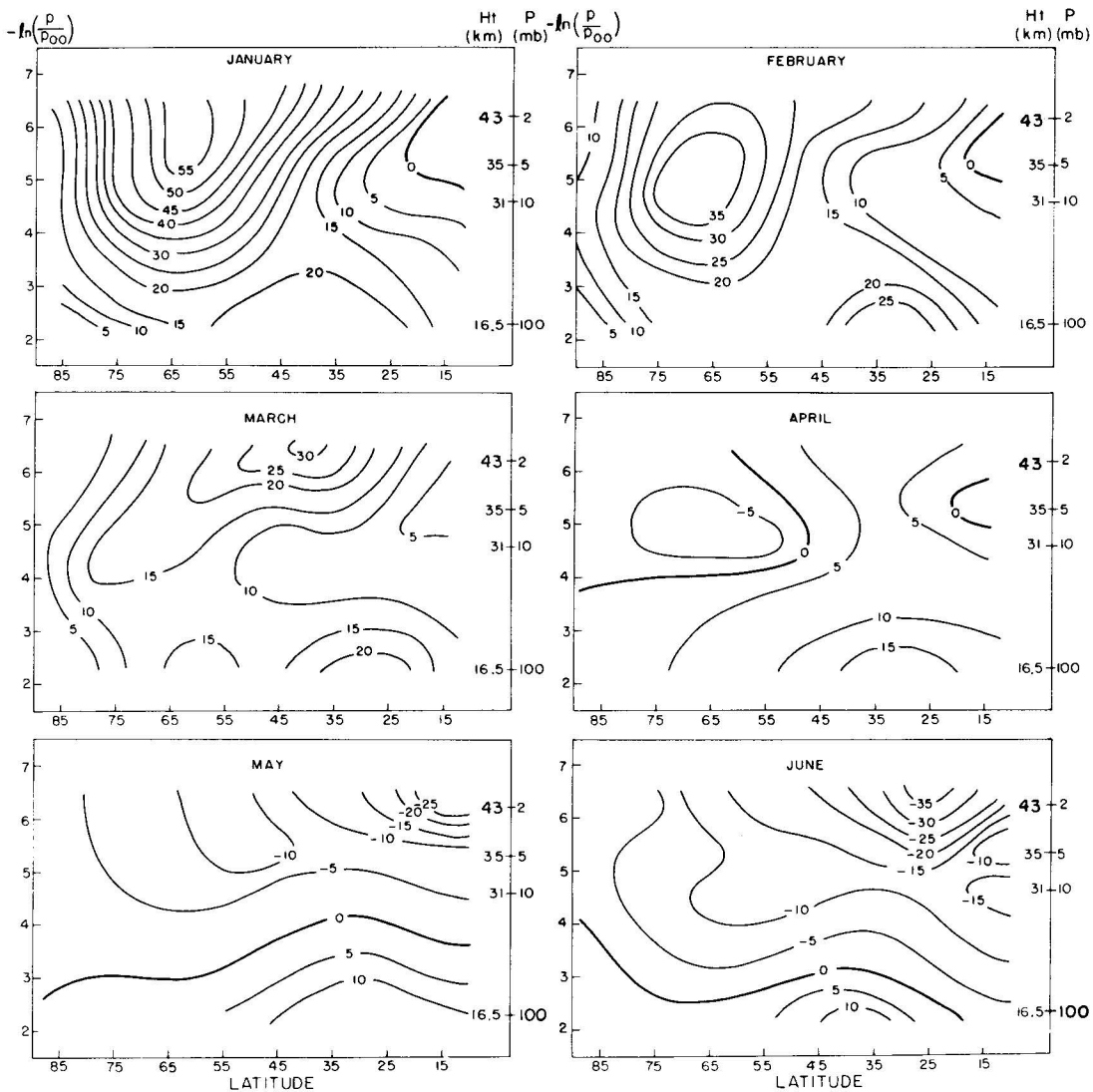


Figure 1. Meridional cross-sections of monthly mean values of zonal wind component. 1972. Units: meters sec<sup>-1</sup>.

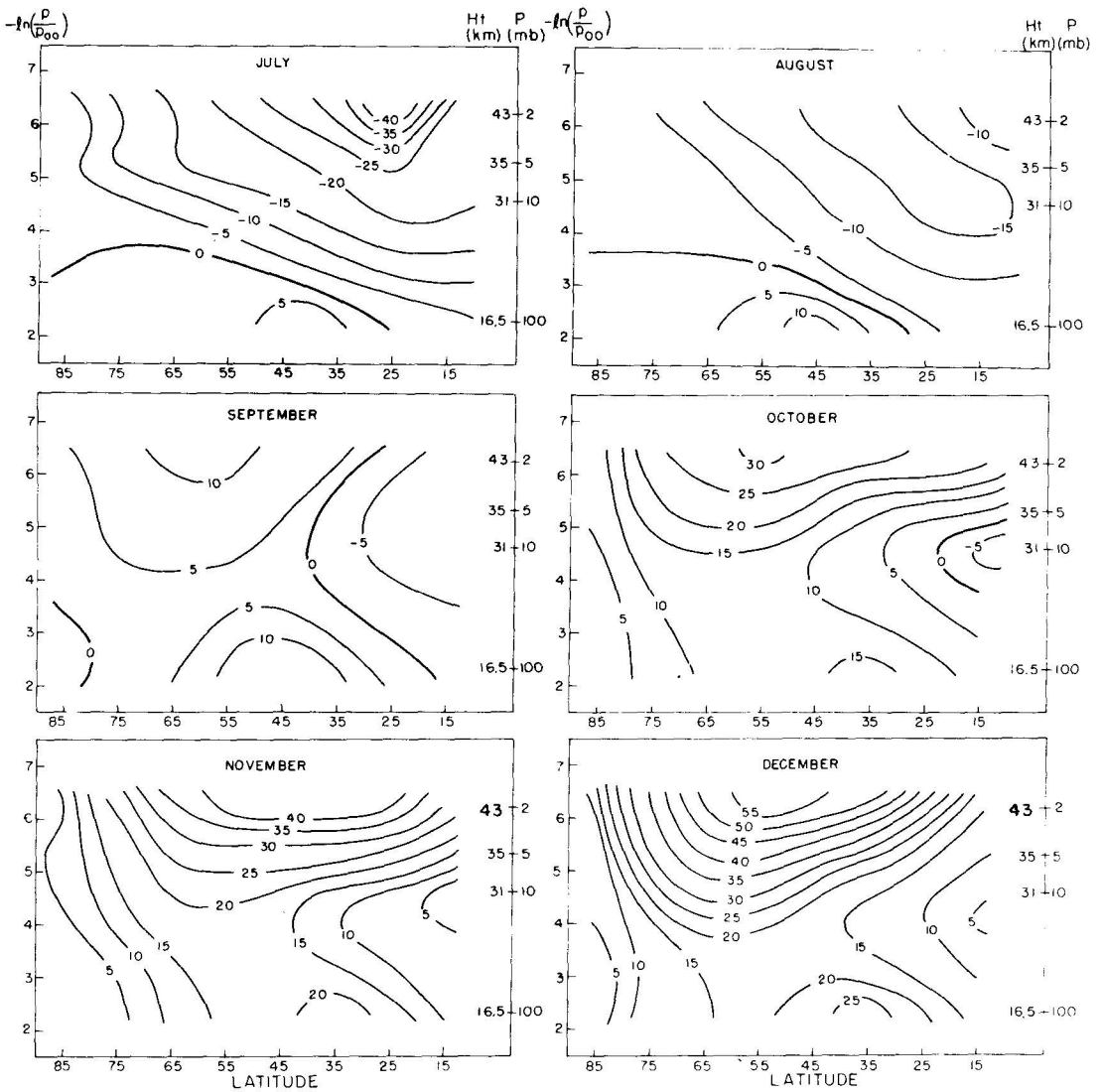


Figure 1. Continued.

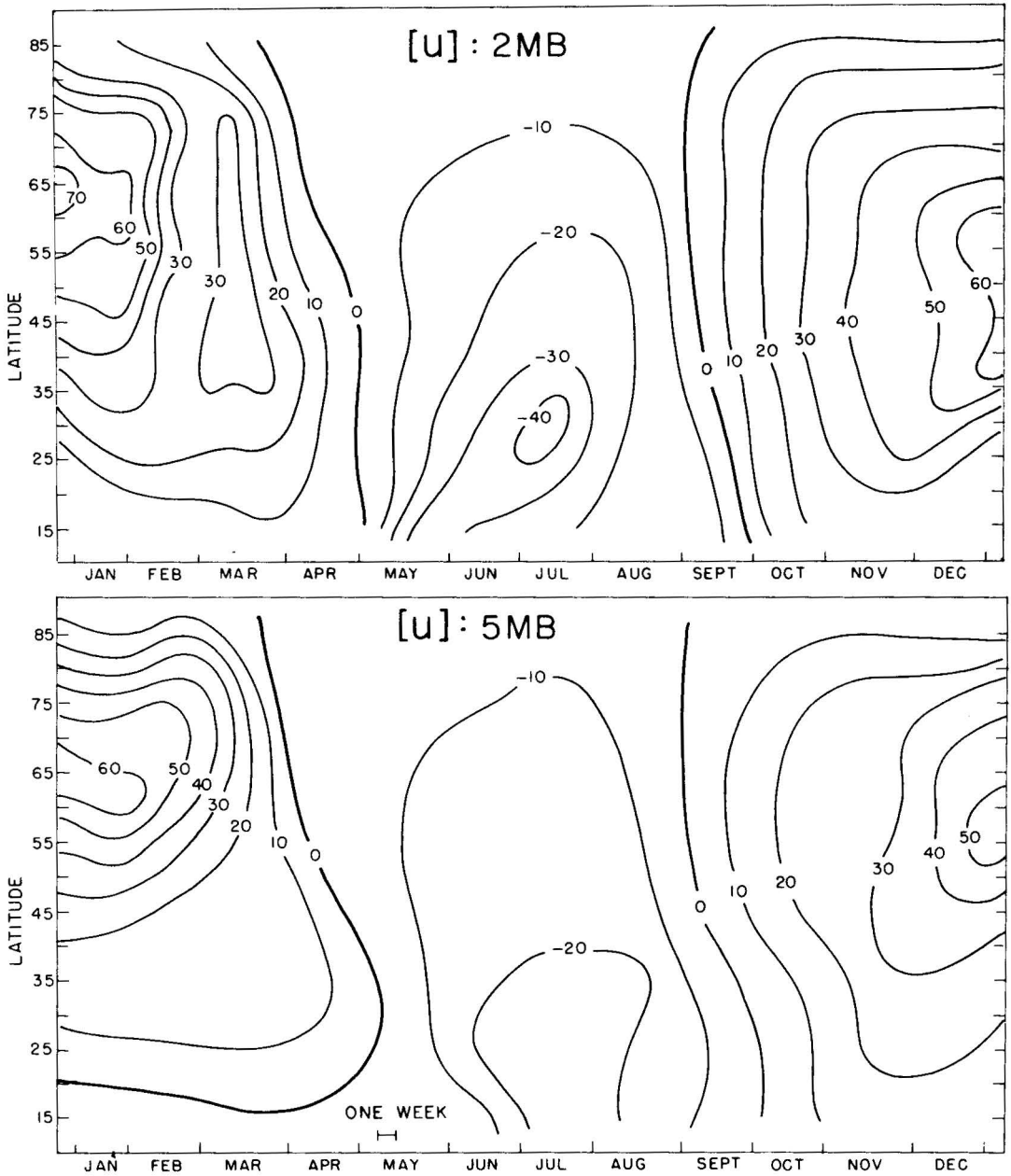


Figure 2. Weekly pattern of zonally averaged zonal wind component at the 2 mb (top) and 5 mb (bottom) levels, 1972. Units: meters  $\text{sec}^{-1}$ .

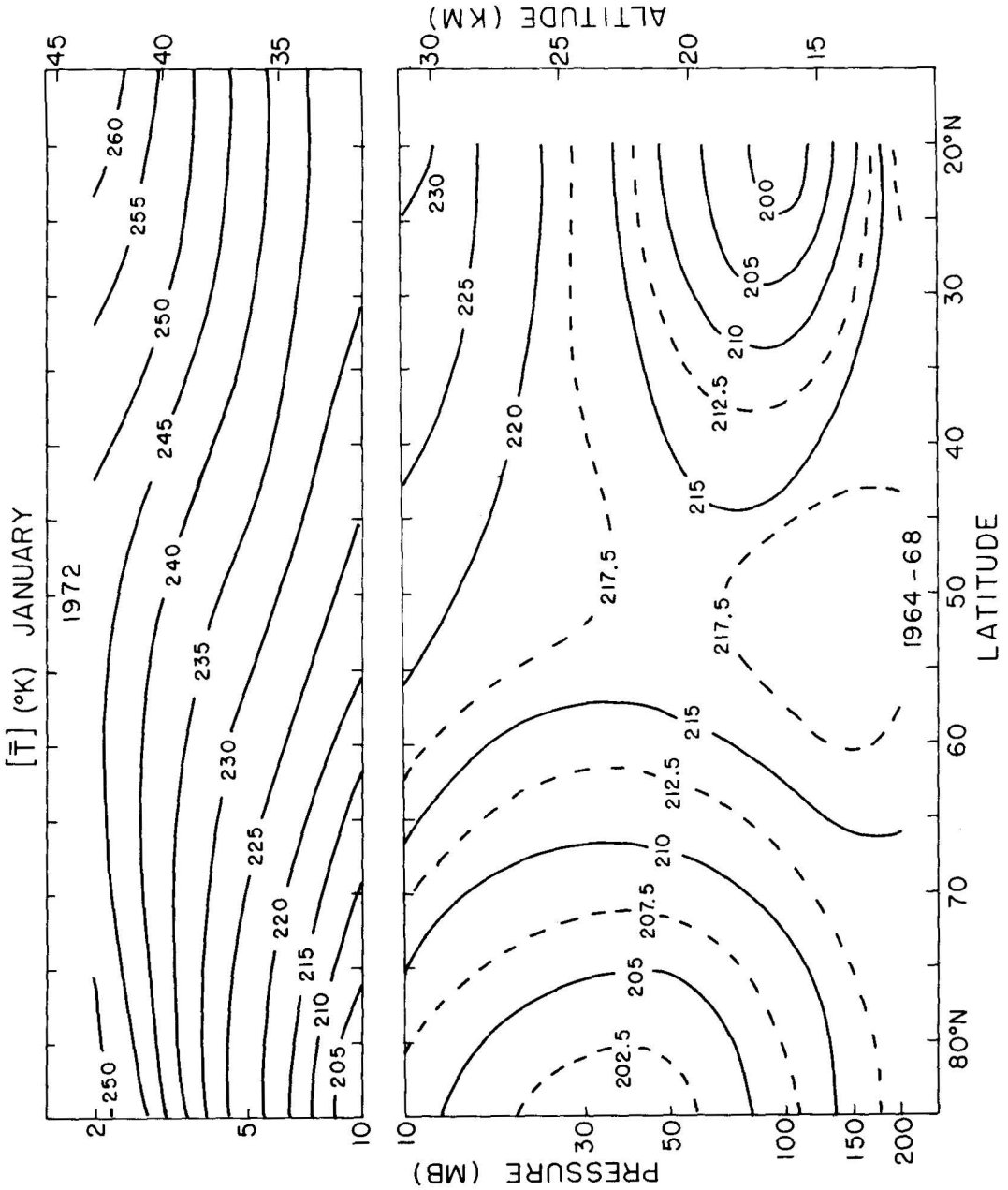


Figure 3. Meridional cross-sections of monthly mean temperature. Top for 1972; bottom for 1964-68. Units: °K.

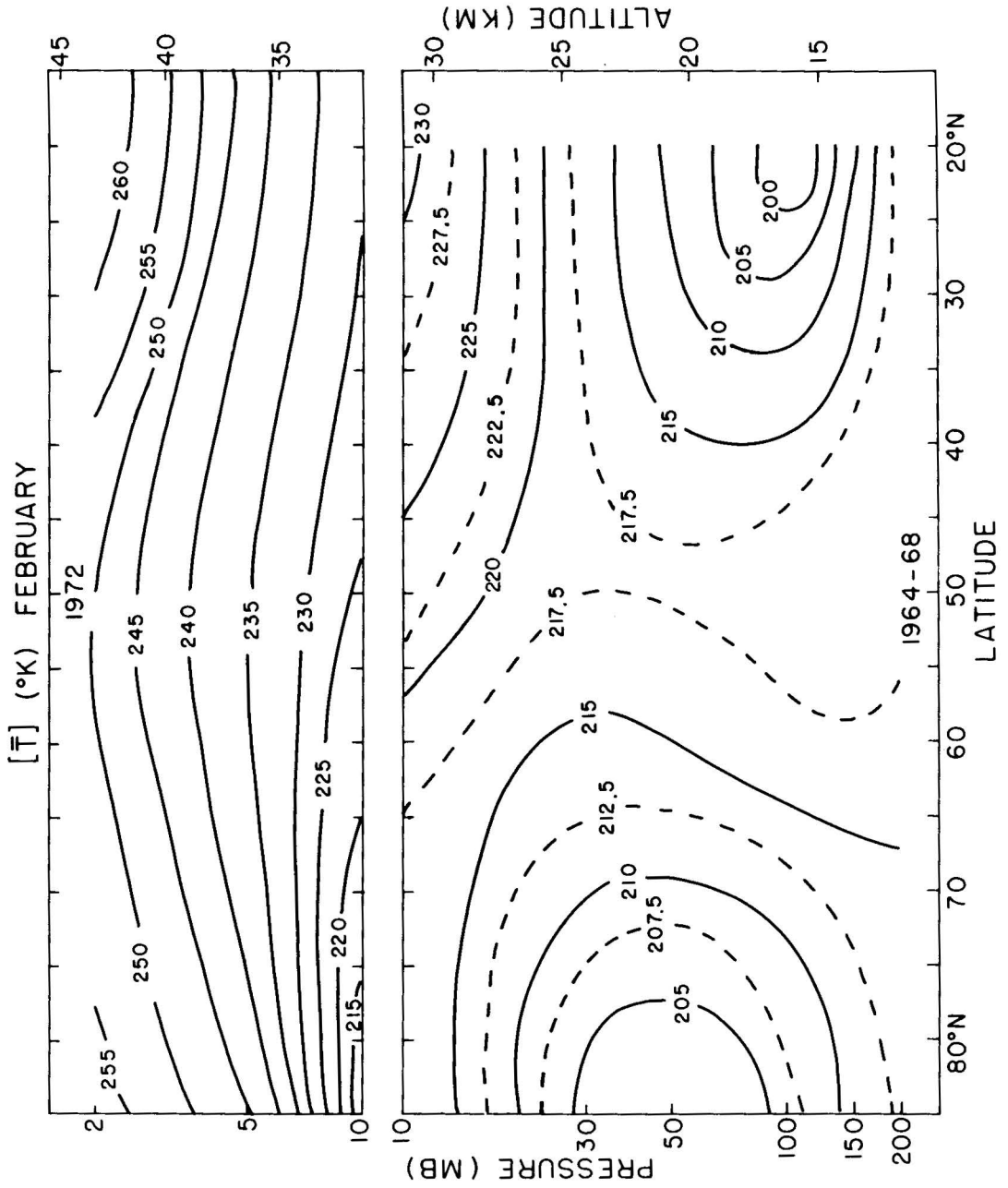


Figure 3. Continued.

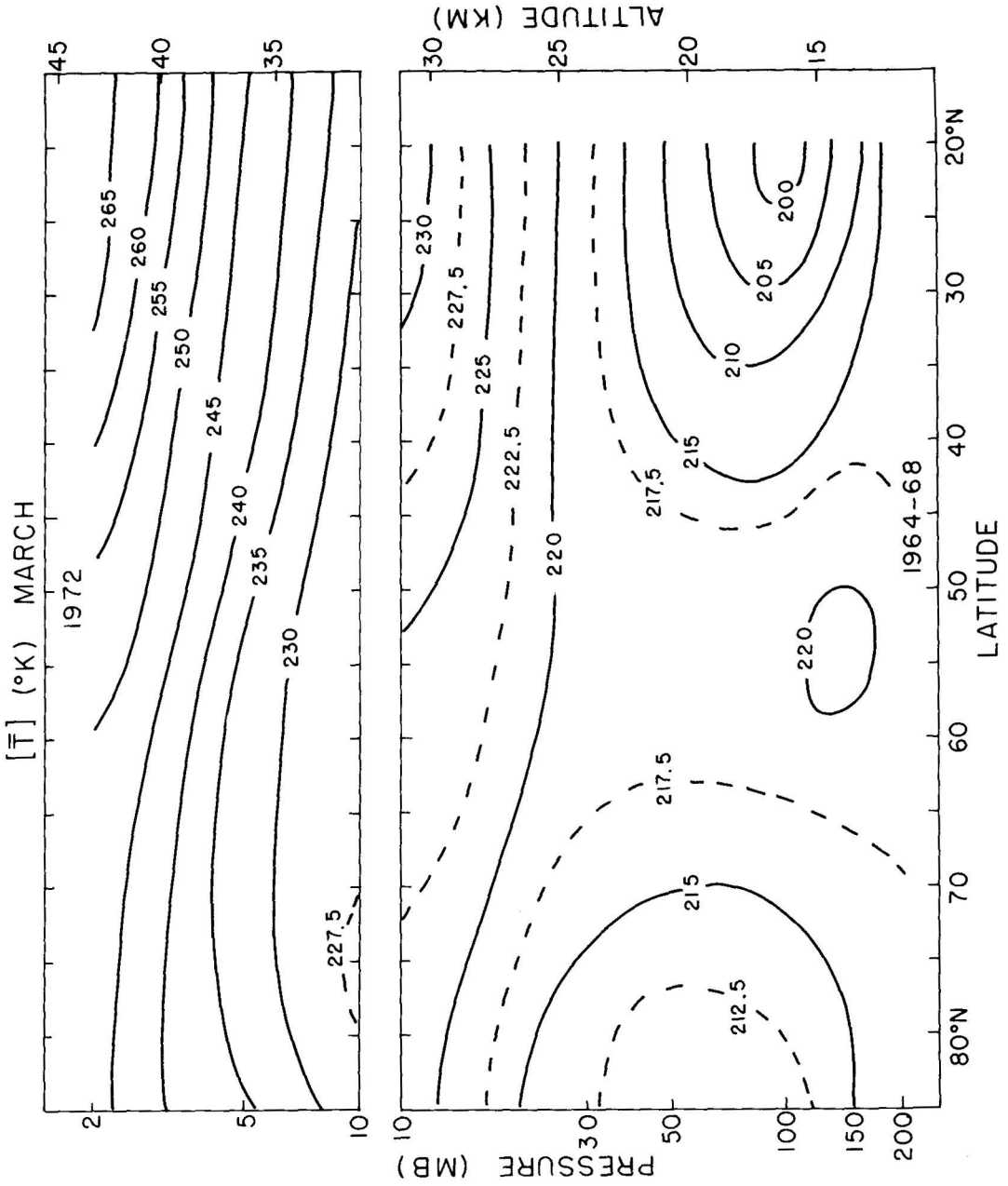


Figure 3. Continued.

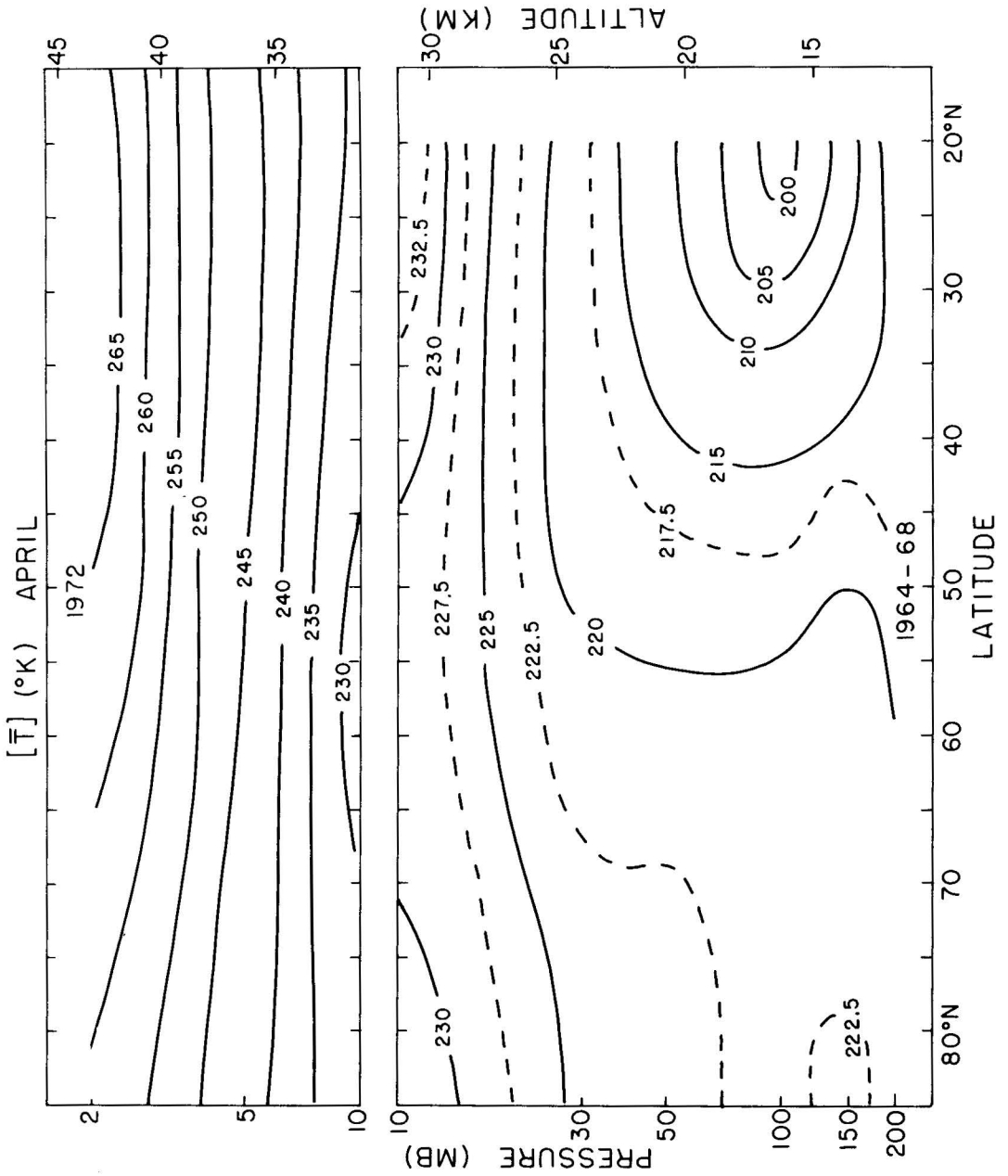


Figure 3. Continued.

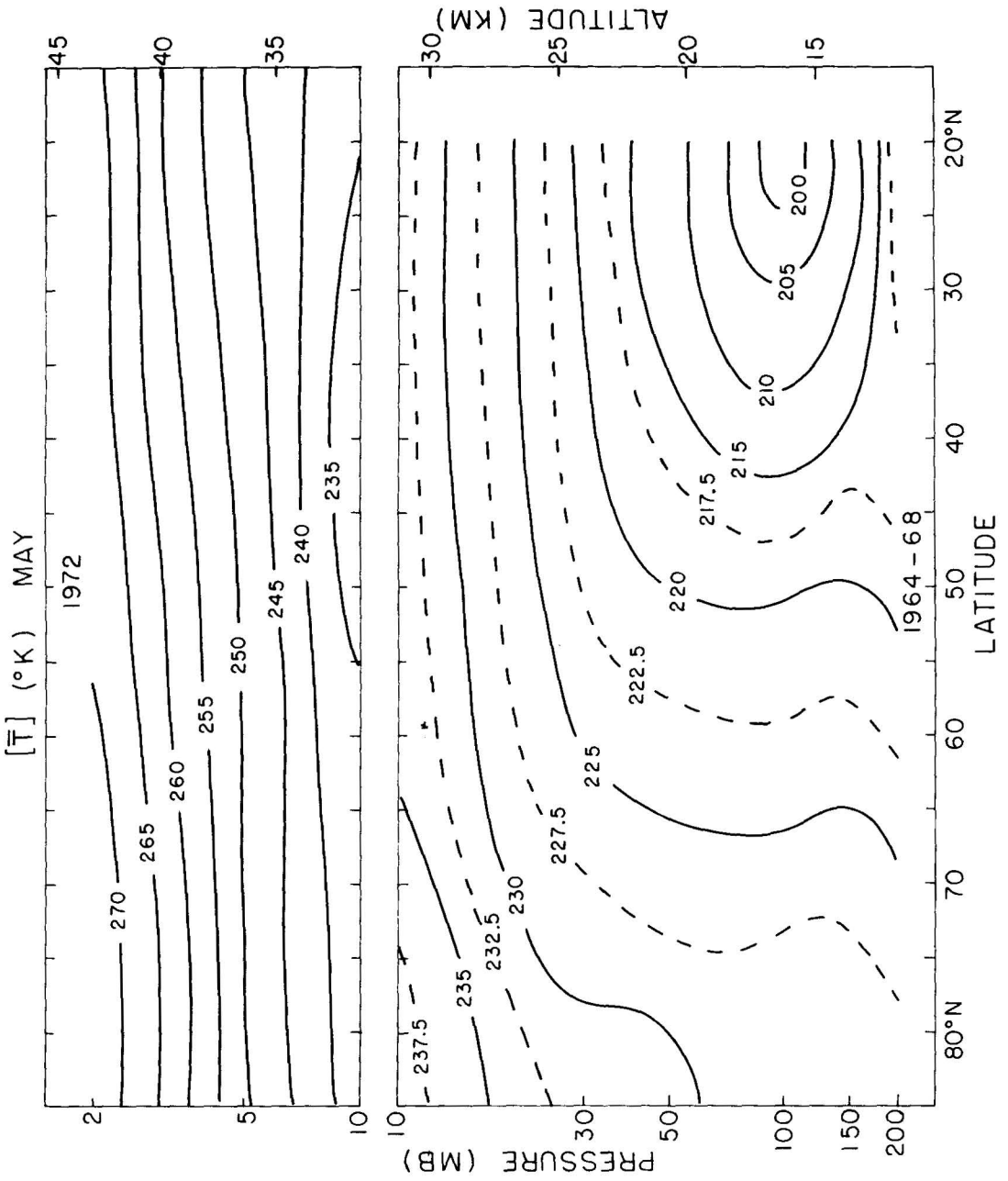


Figure 3. Continued.

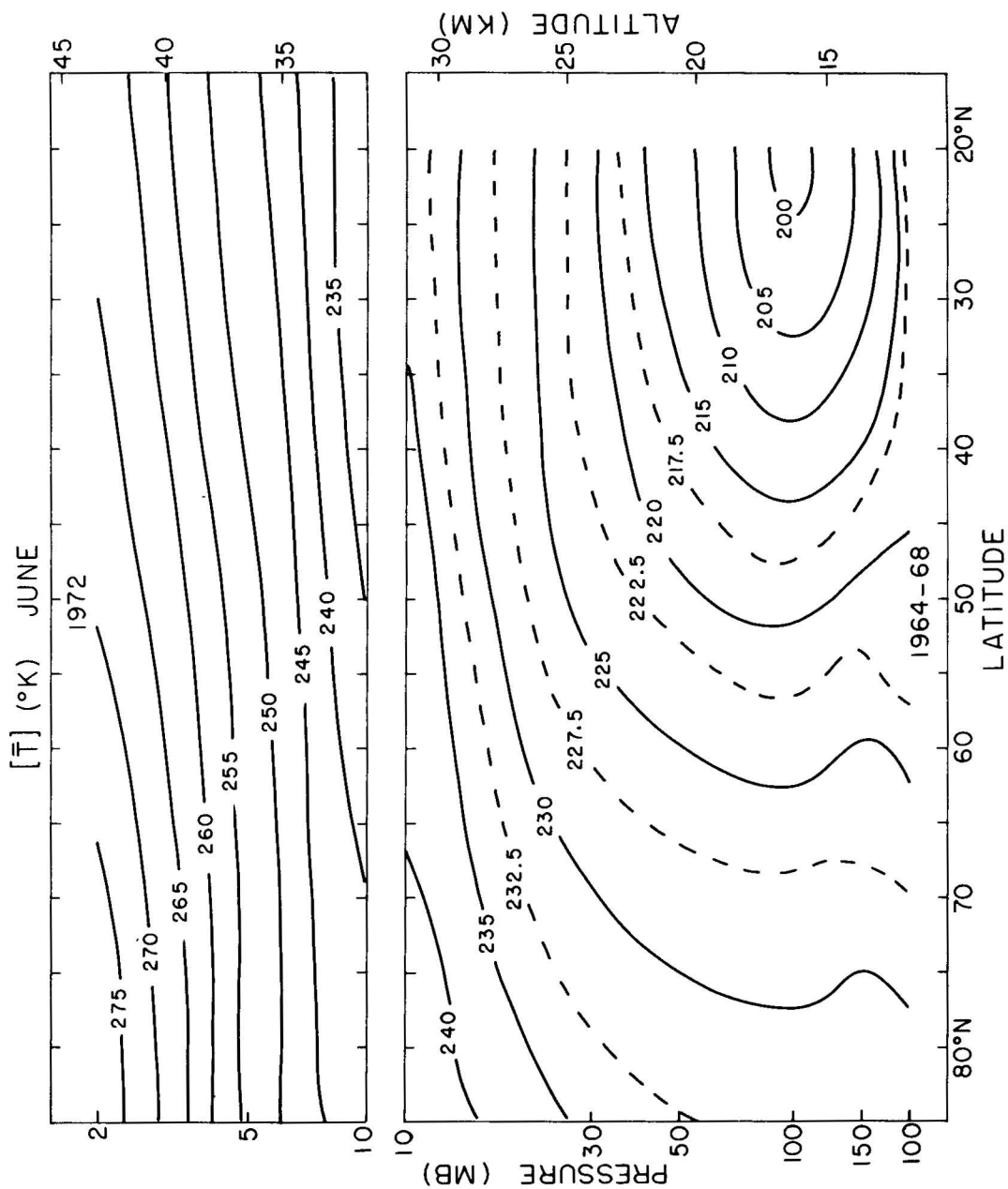


Figure 3. Continued.

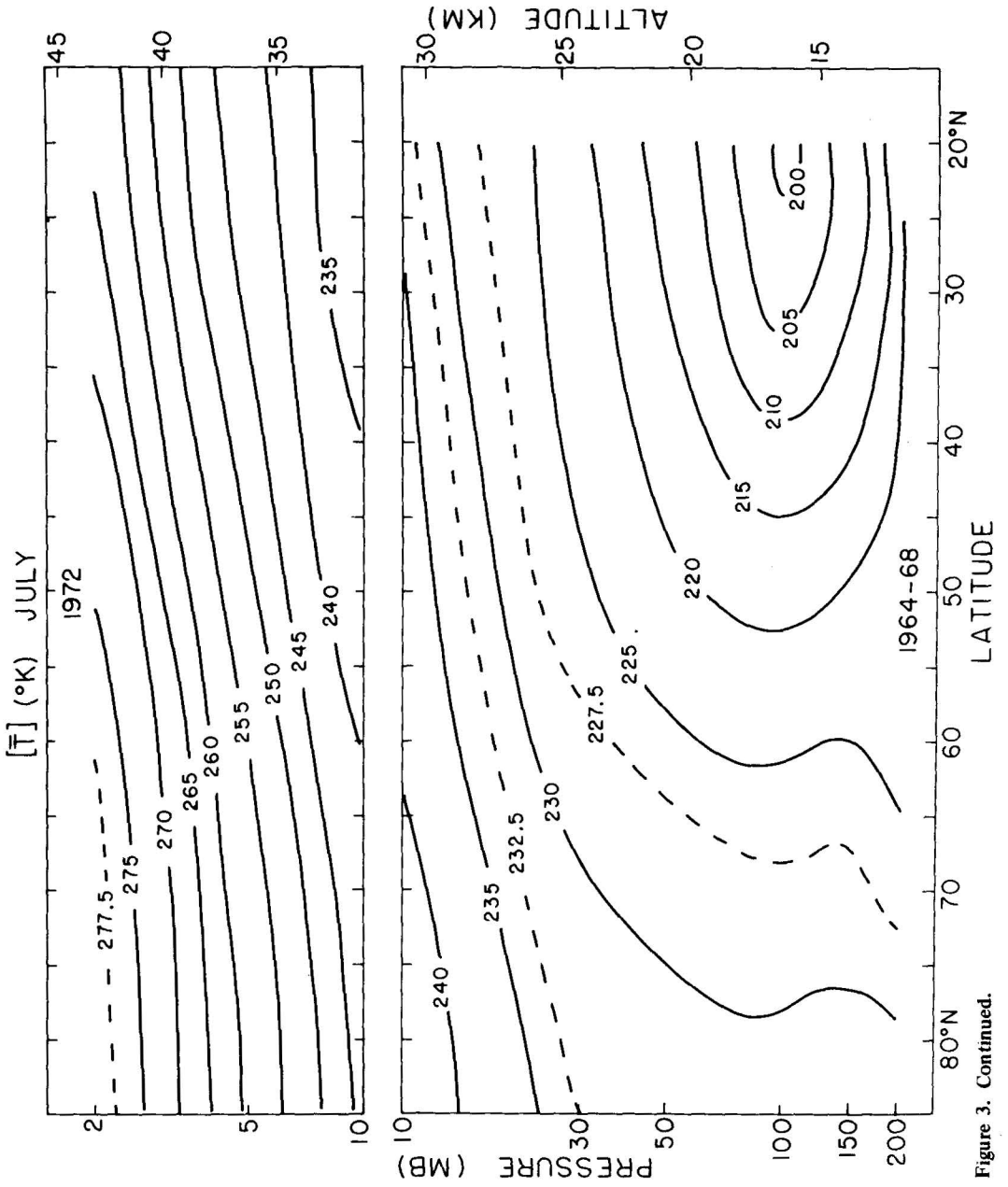


Figure 3. Continued.

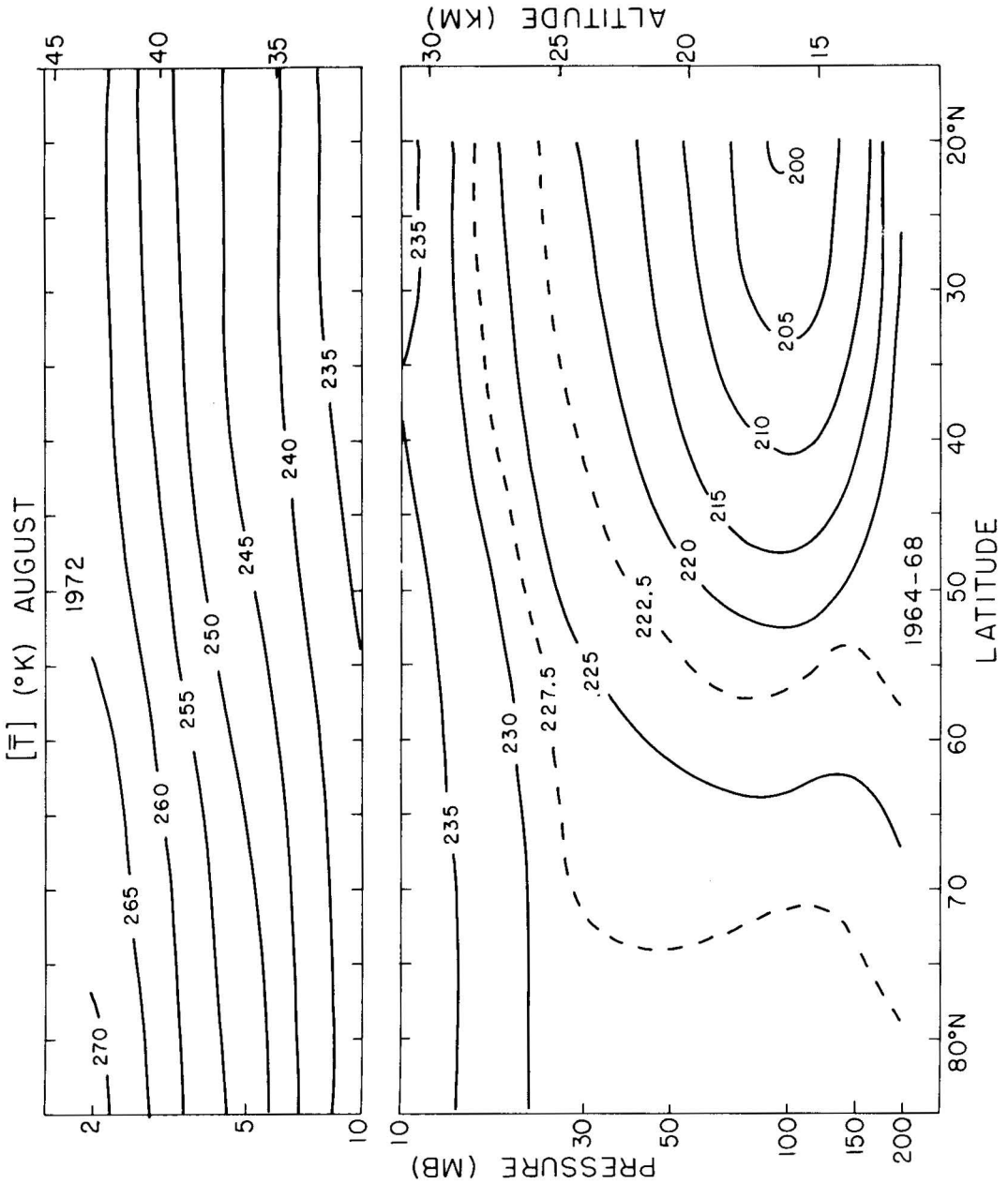


Figure 3. Continued.

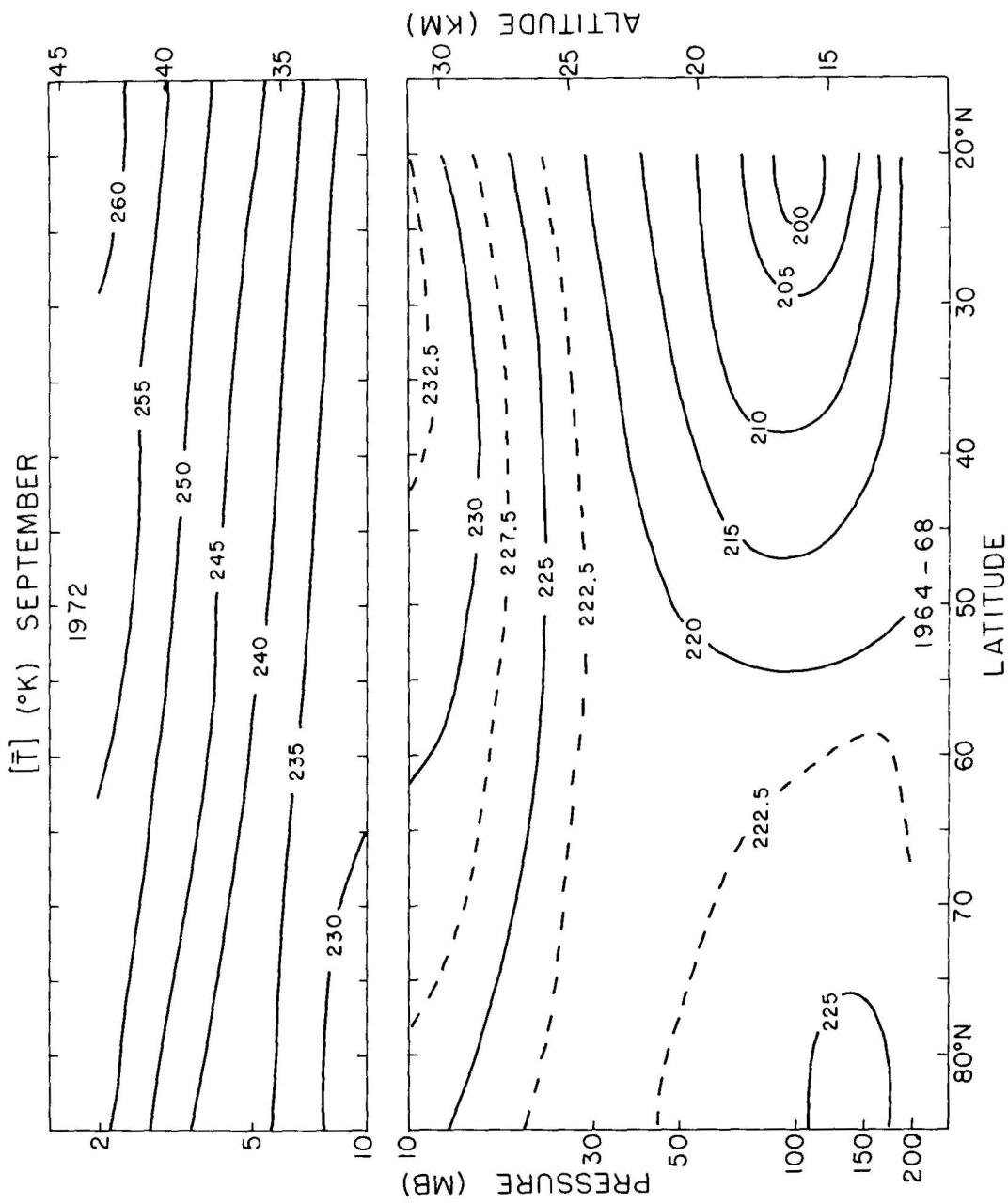


Figure 3. Continued.

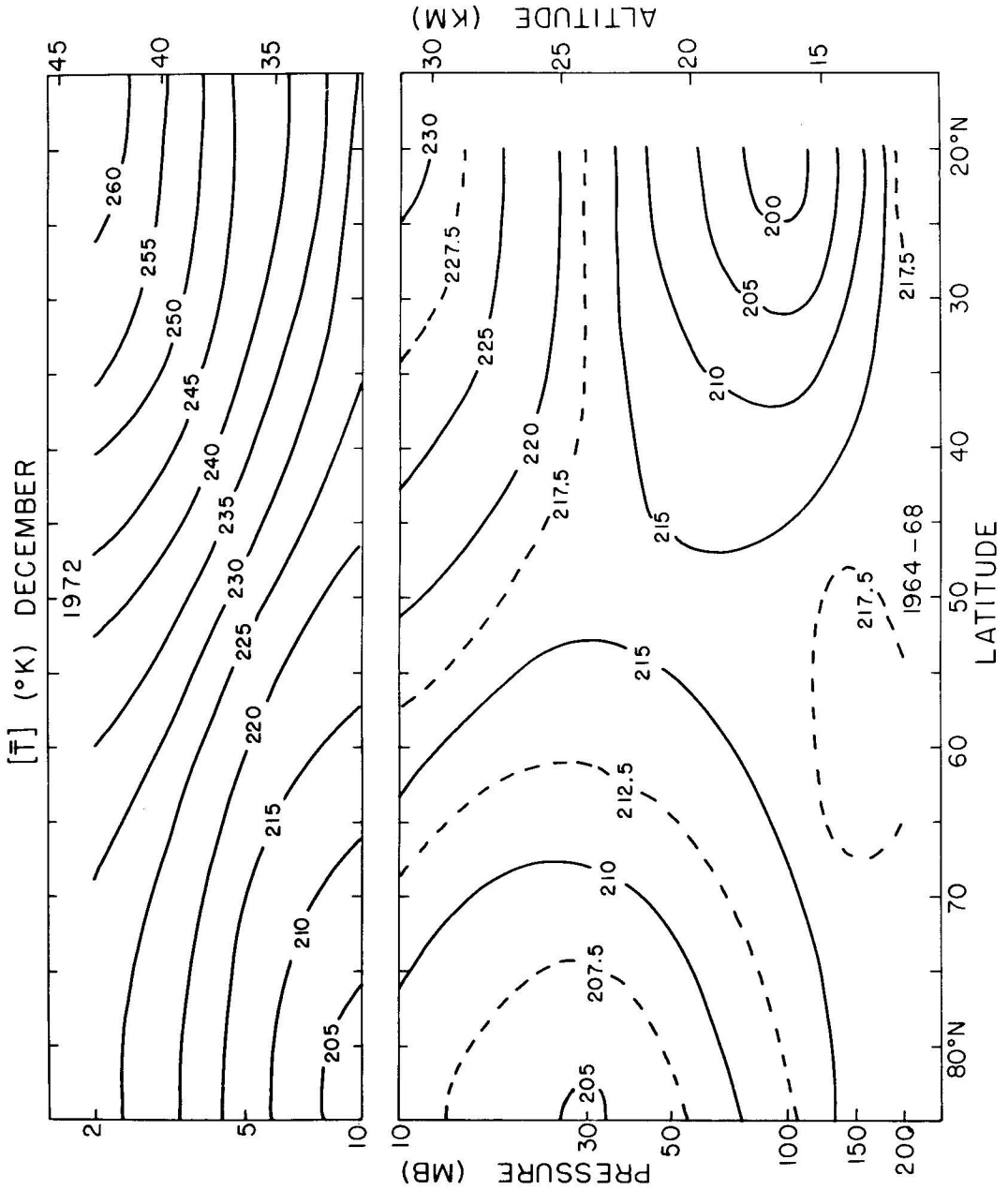


Figure 3. Continued.

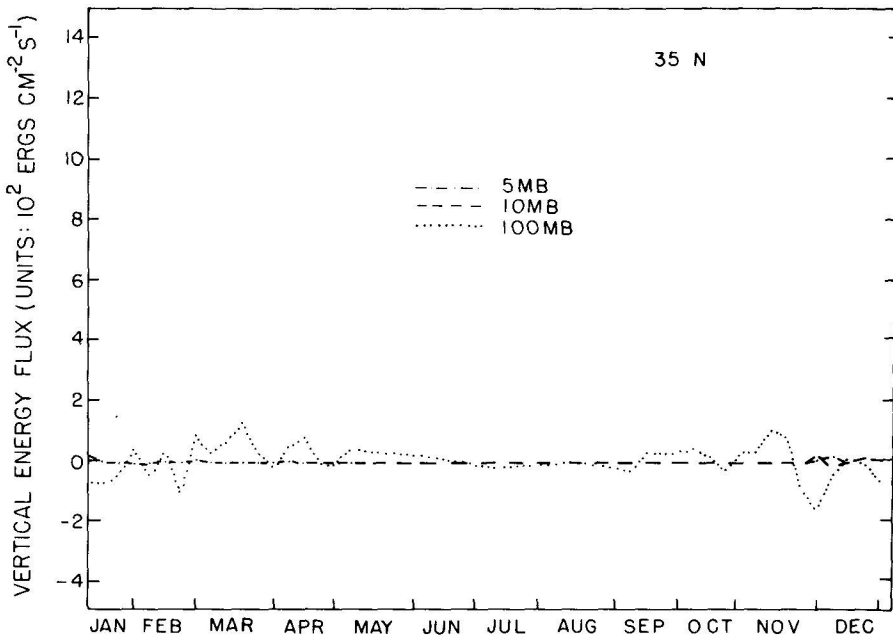
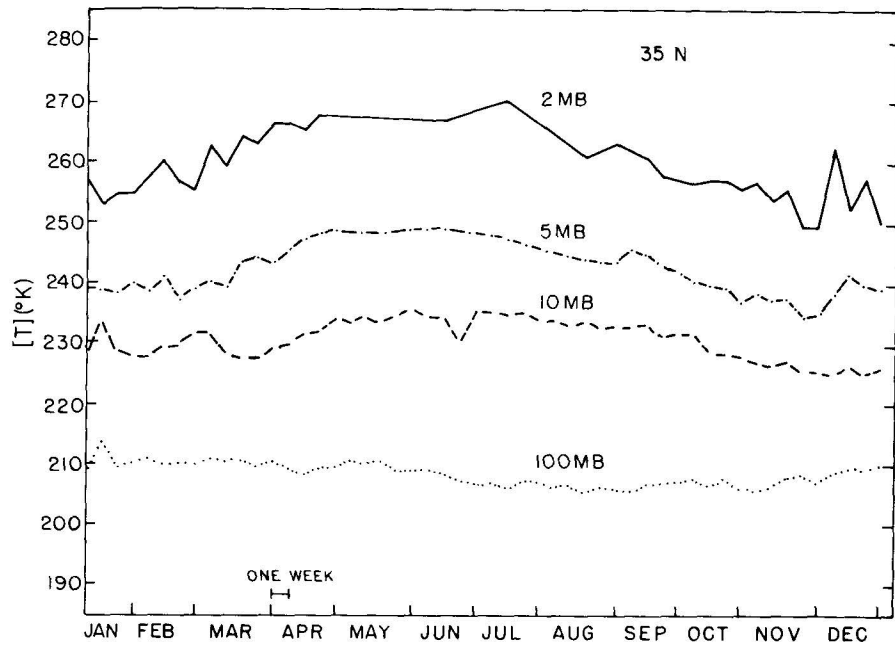


Figure 4. Weekly pattern of zonally averaged temperature,  $[T]$ , in units of  $^{\circ}\text{K}$ , and vertical energy flux [pw], in units of  $\text{ergs cm}^{-2} \text{sec}^{-1}$ , at latitudes from  $35^{\circ}\text{N}$  to  $85^{\circ}\text{N}$ .

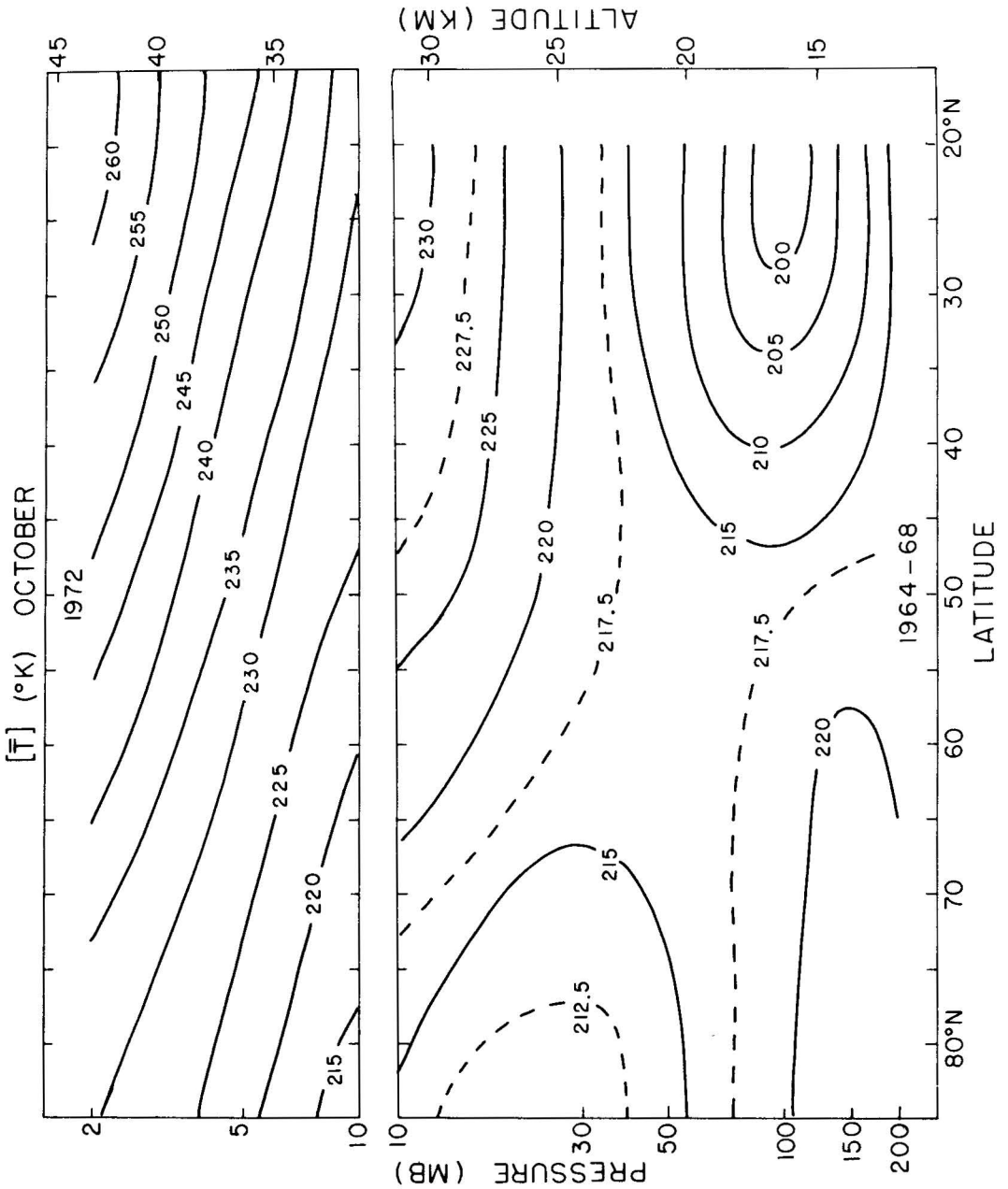


Figure 3. Continued.

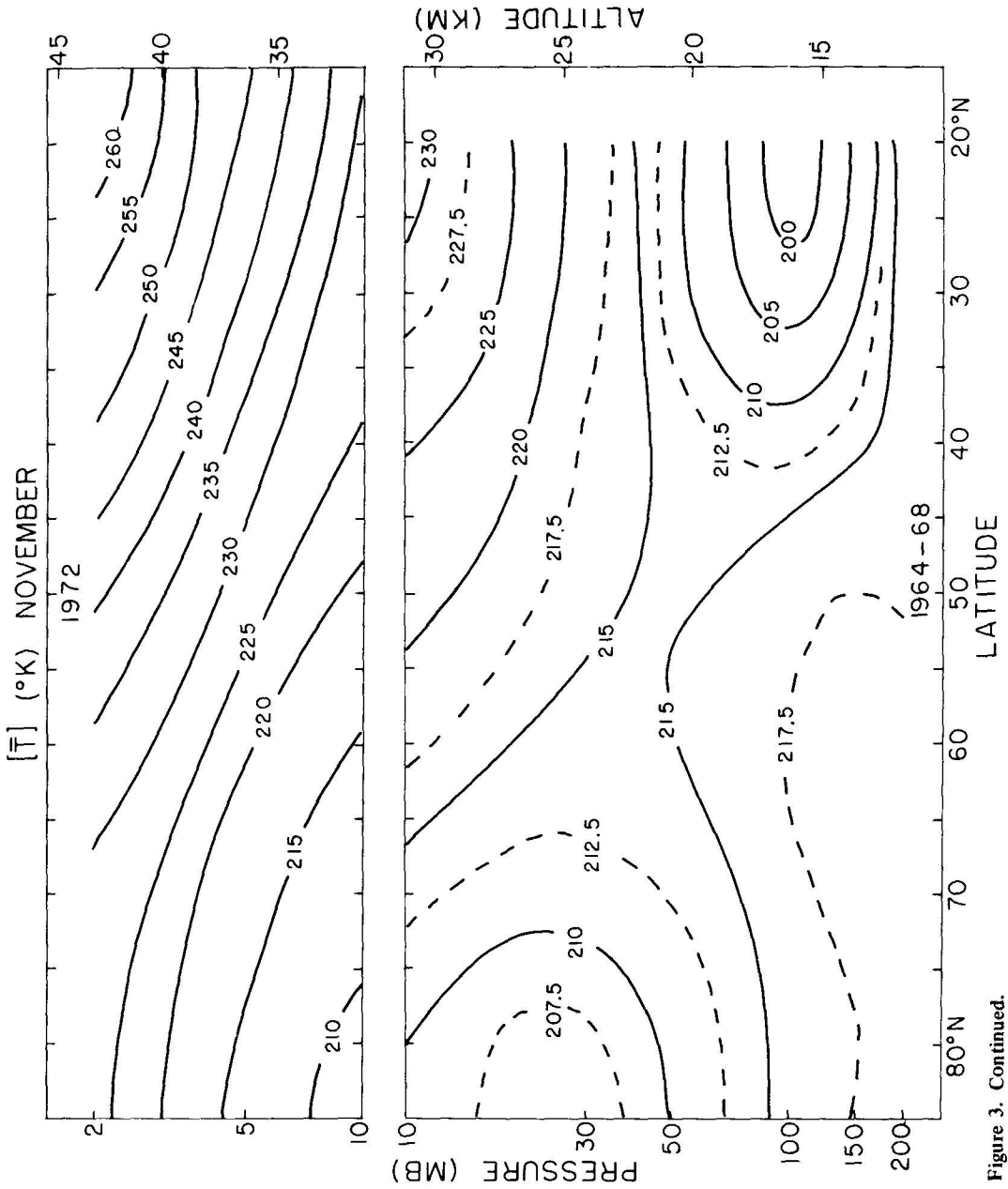


Figure 3. Continued.

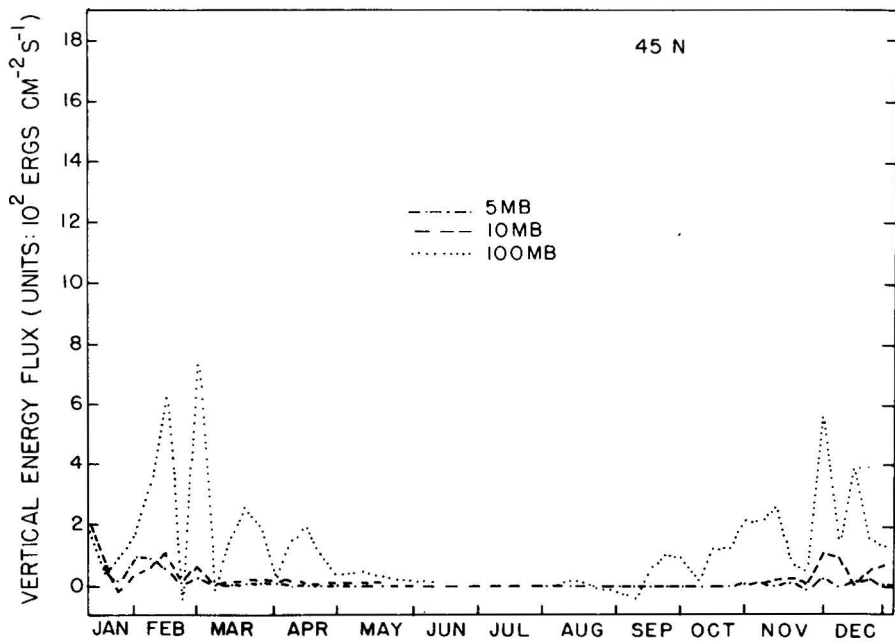
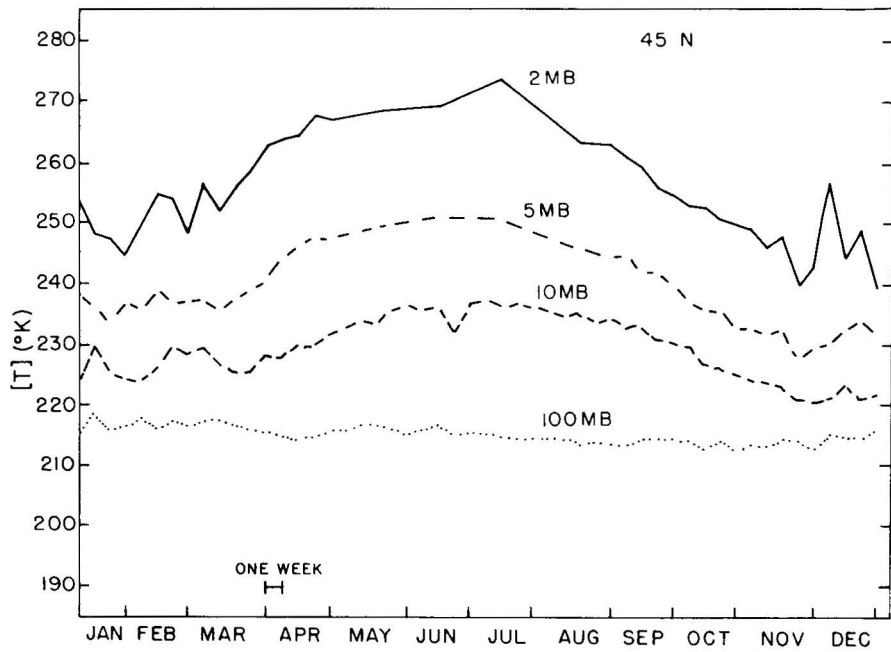


Figure 4. Continued.

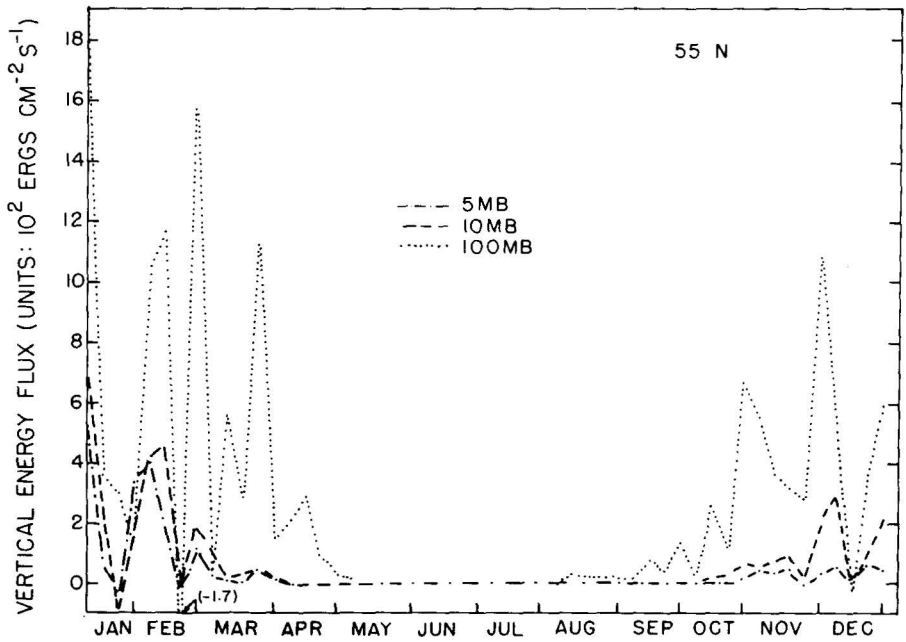
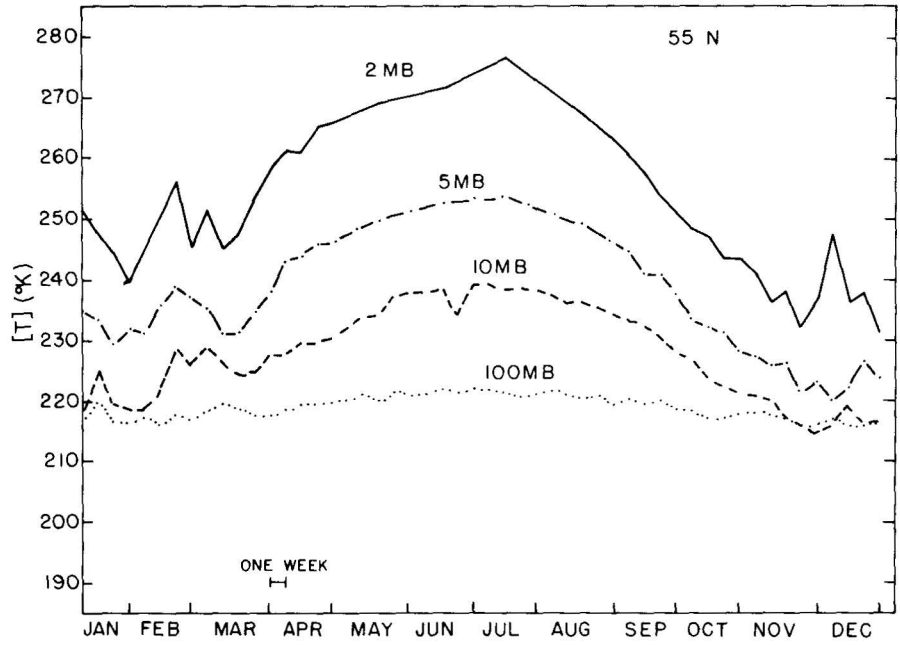


Figure 4. Continued.

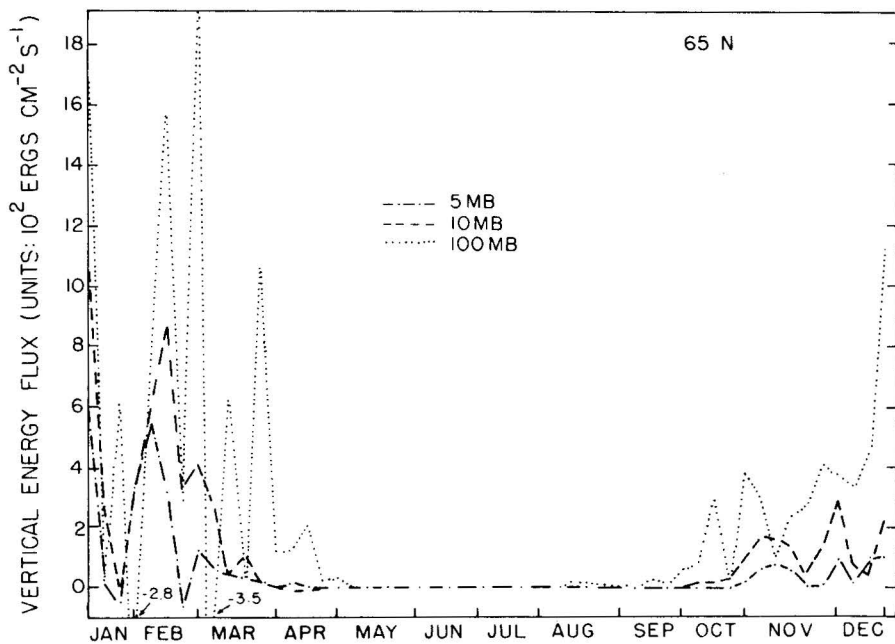
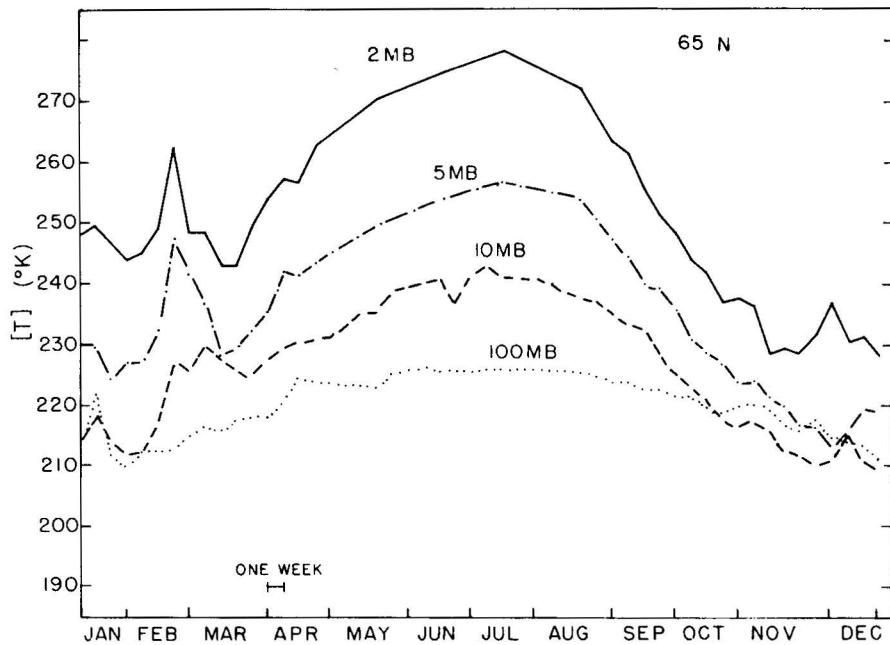


Figure 4. Continued.

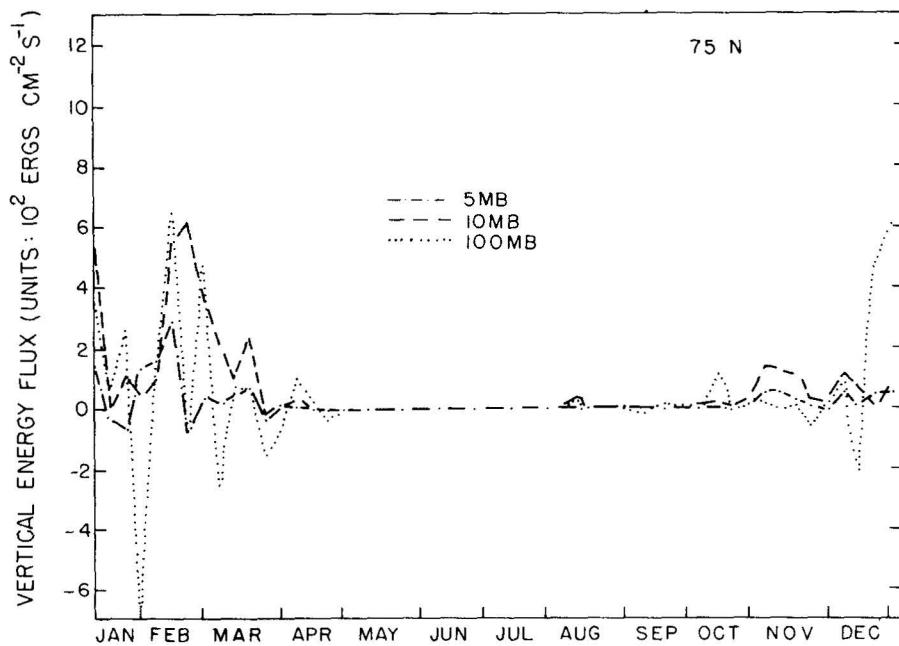
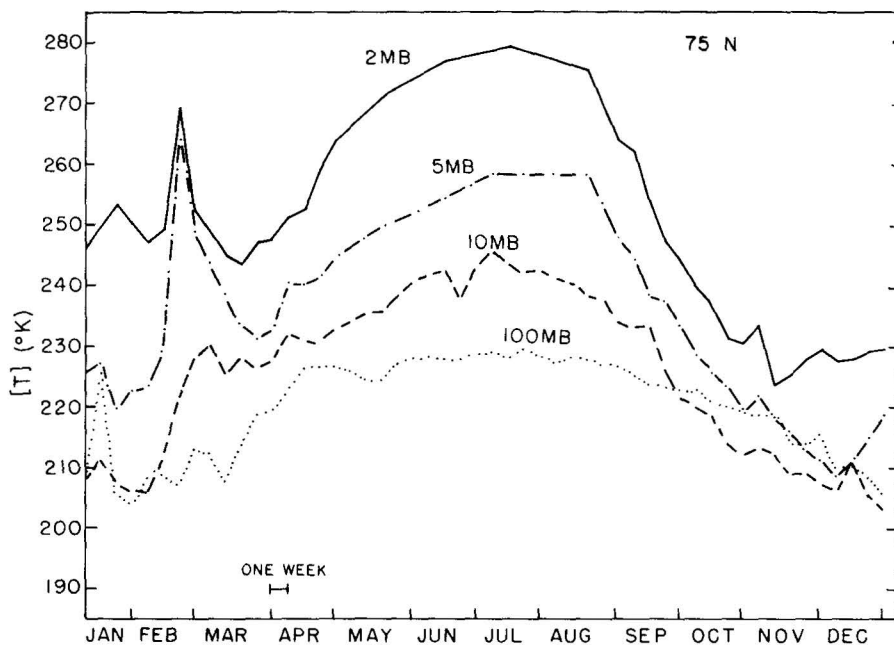


Figure 4. Continued.

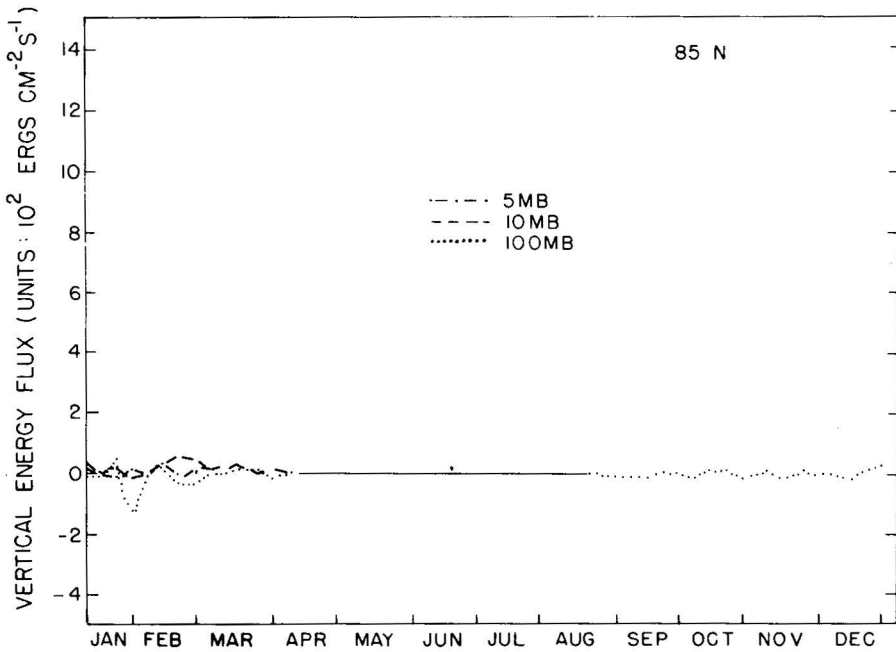
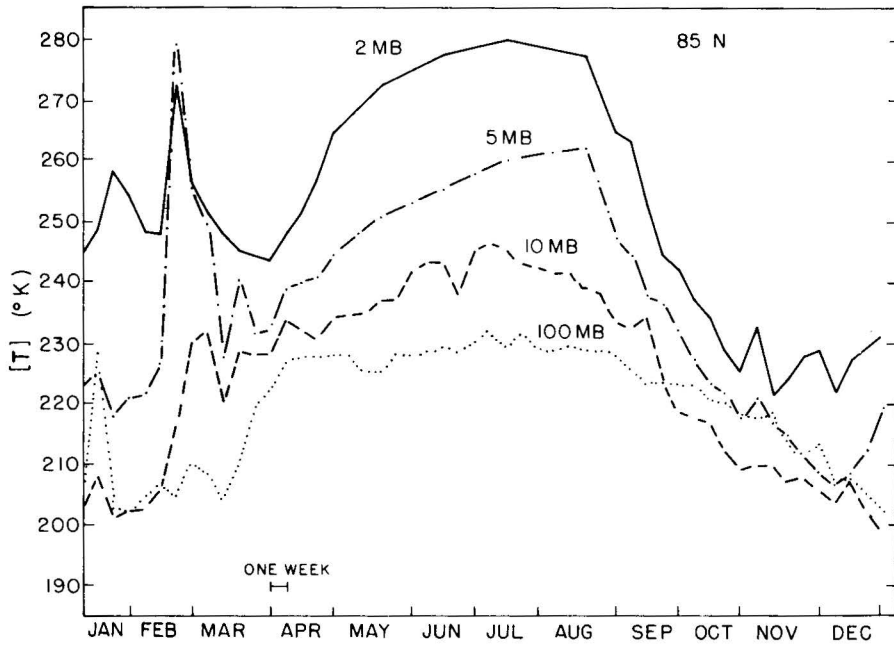


Figure 4. Continued.

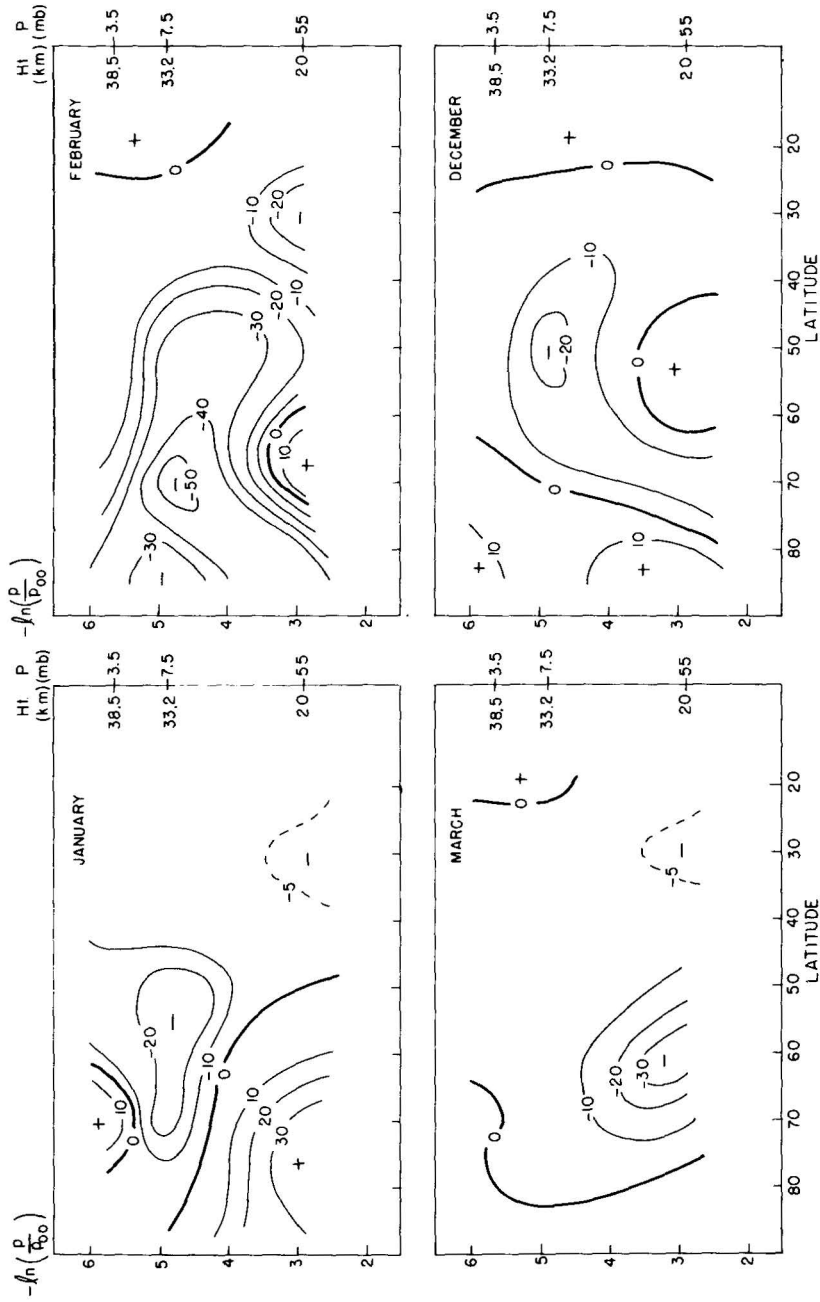


Figure 5. Meridional cross-sections of total energy flux divergence for selected months (positive numbers indicate divergence). Units:  $10^{-5} \text{ ergs cm}^{-3} \text{ sec}^{-1}$ .

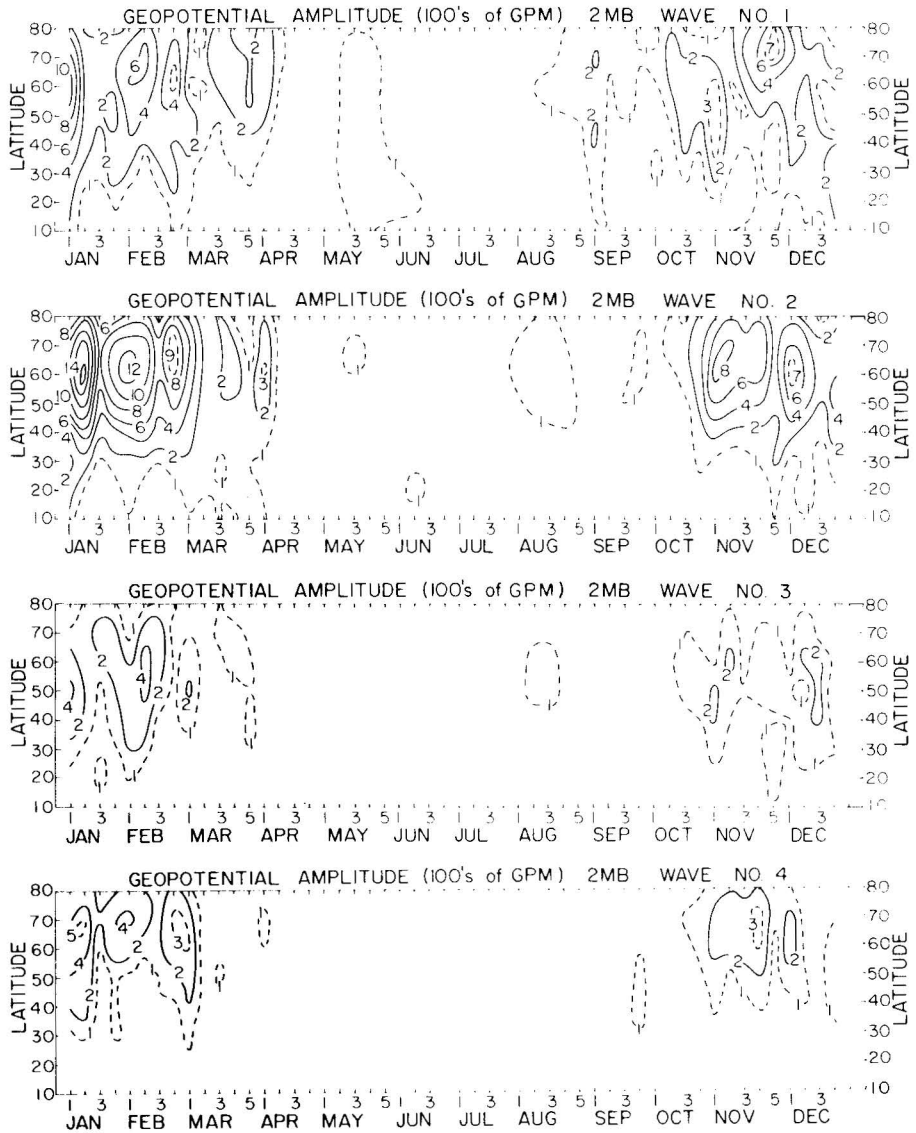


Figure 6. Weekly pattern of geopotential amplitude (in 100's of GPM) versus latitude. Wave numbers 1-4 for 2 mb and 1 and 2 for 5, 10, and 100 mb.

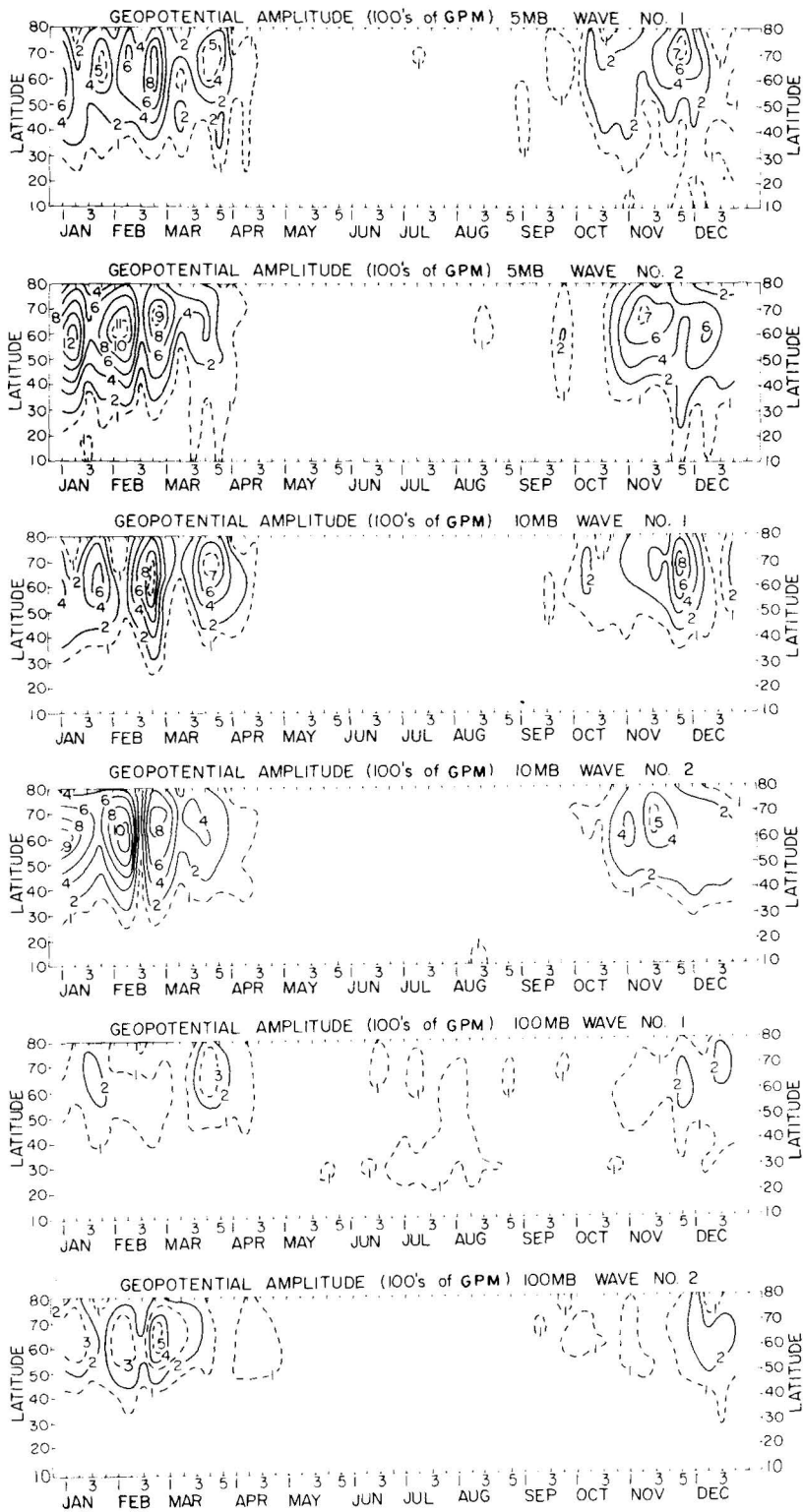


Figure 6. Continued.

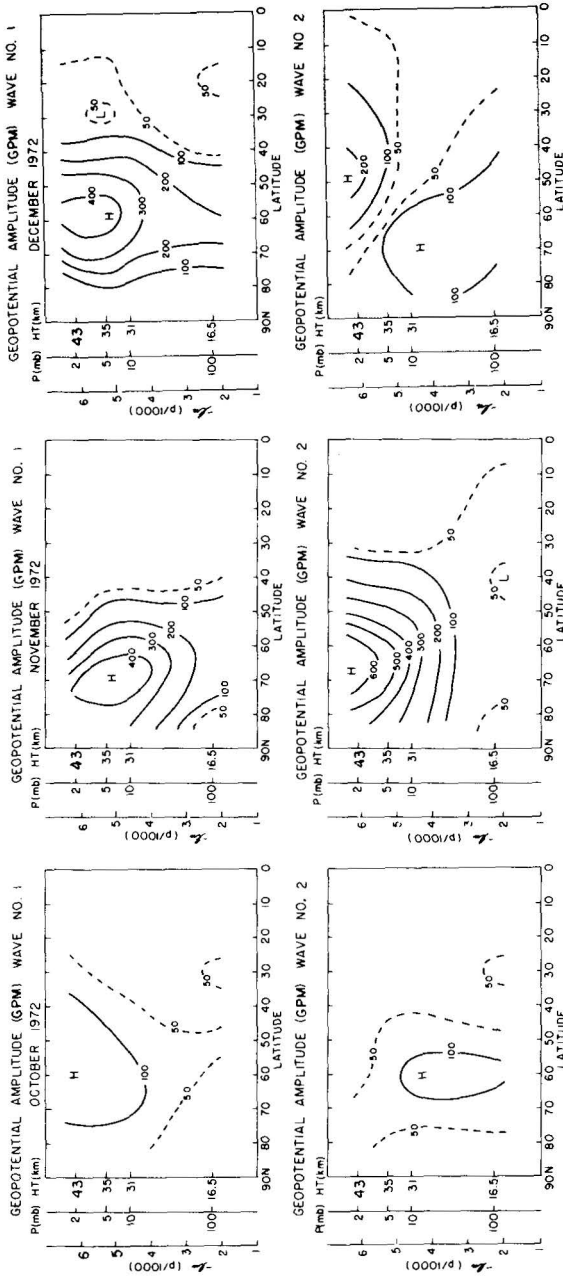


Figure 7. Meridional cross-sections of monthly mean geopotential amplitude (in GPM) for the winter months for wave numbers 1 and 2.

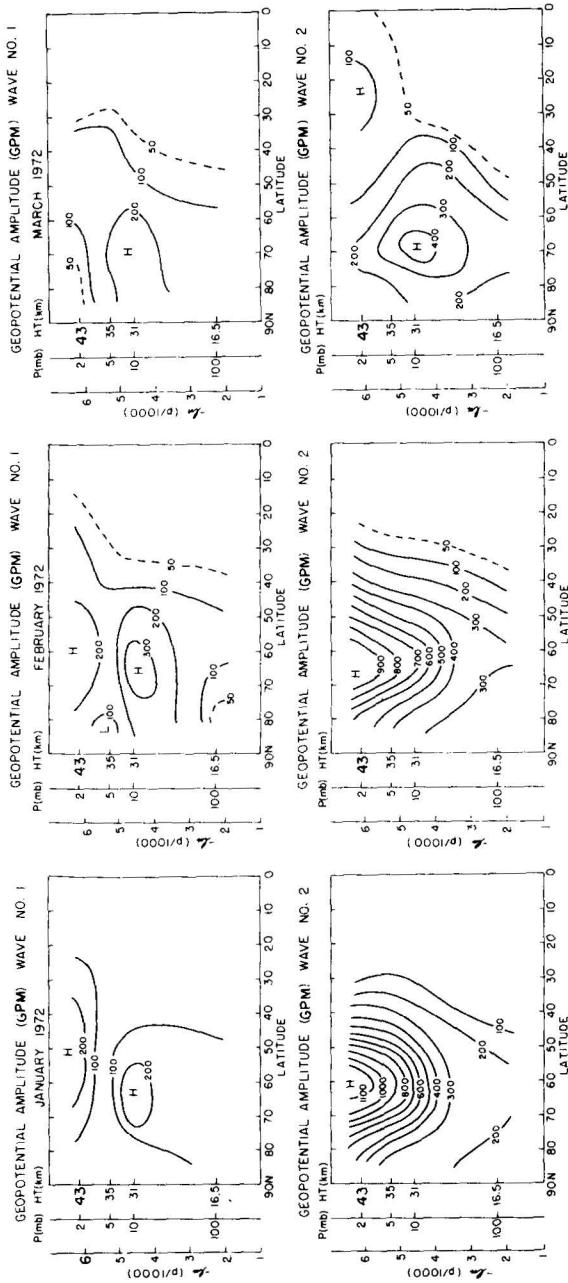


Figure 7. Continued.



PHASE ANGLE 60 N WAVE NO. 1 1972

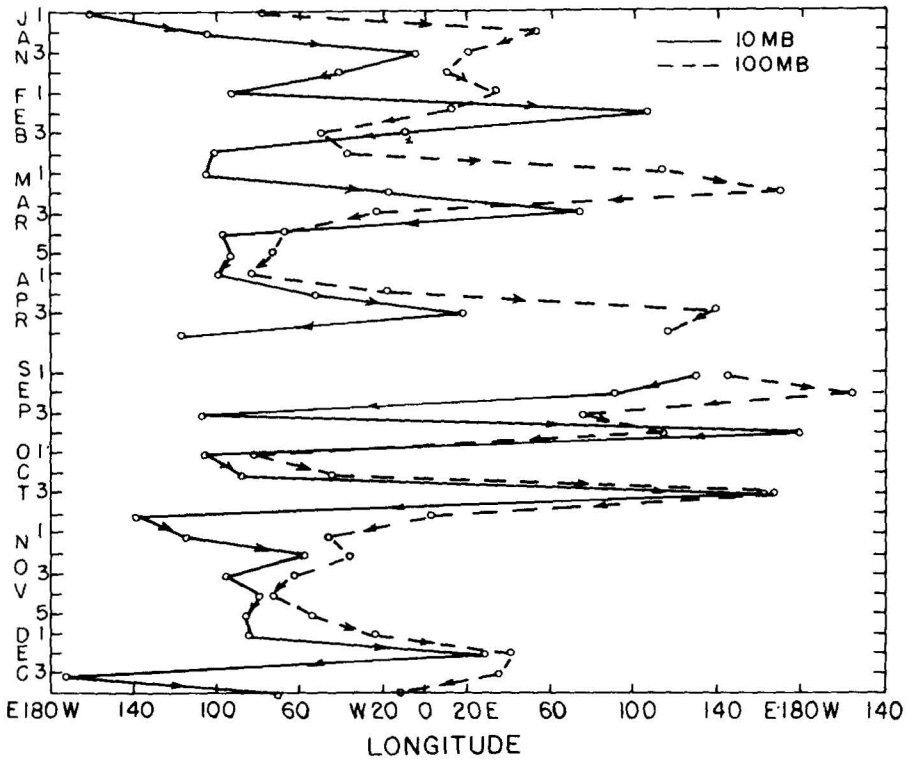
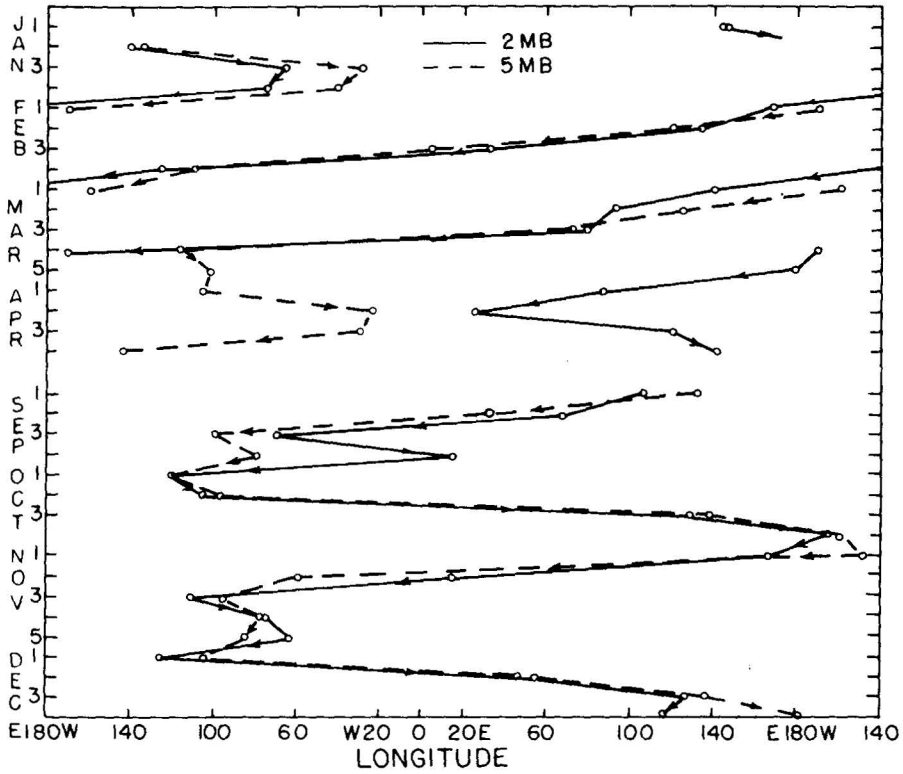


Figure 9. Longitude of phase angle at 60°N for 2, 5, 10 and 100 mb for wave numbers 1 and 2.

PHASE ANGLE 60 N WAVE NO. 2 1972

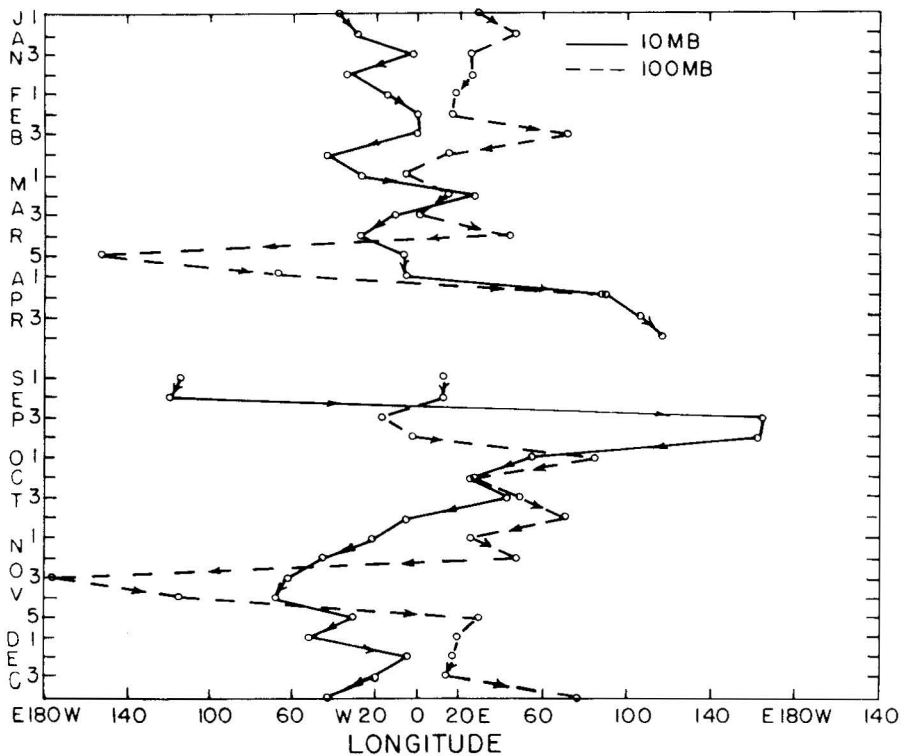
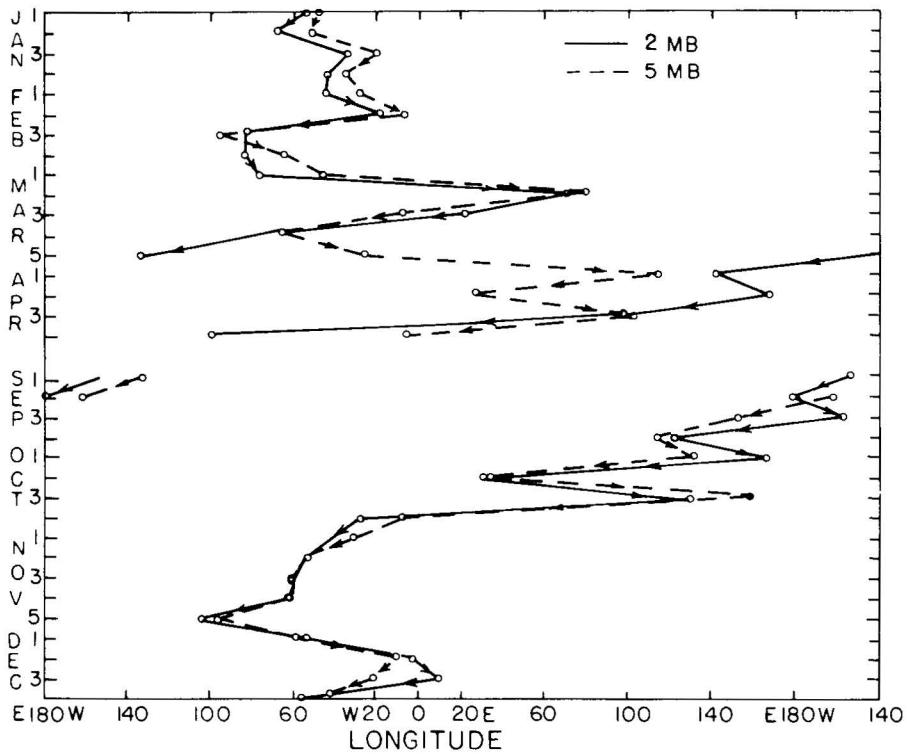


Figure 9. Continued.

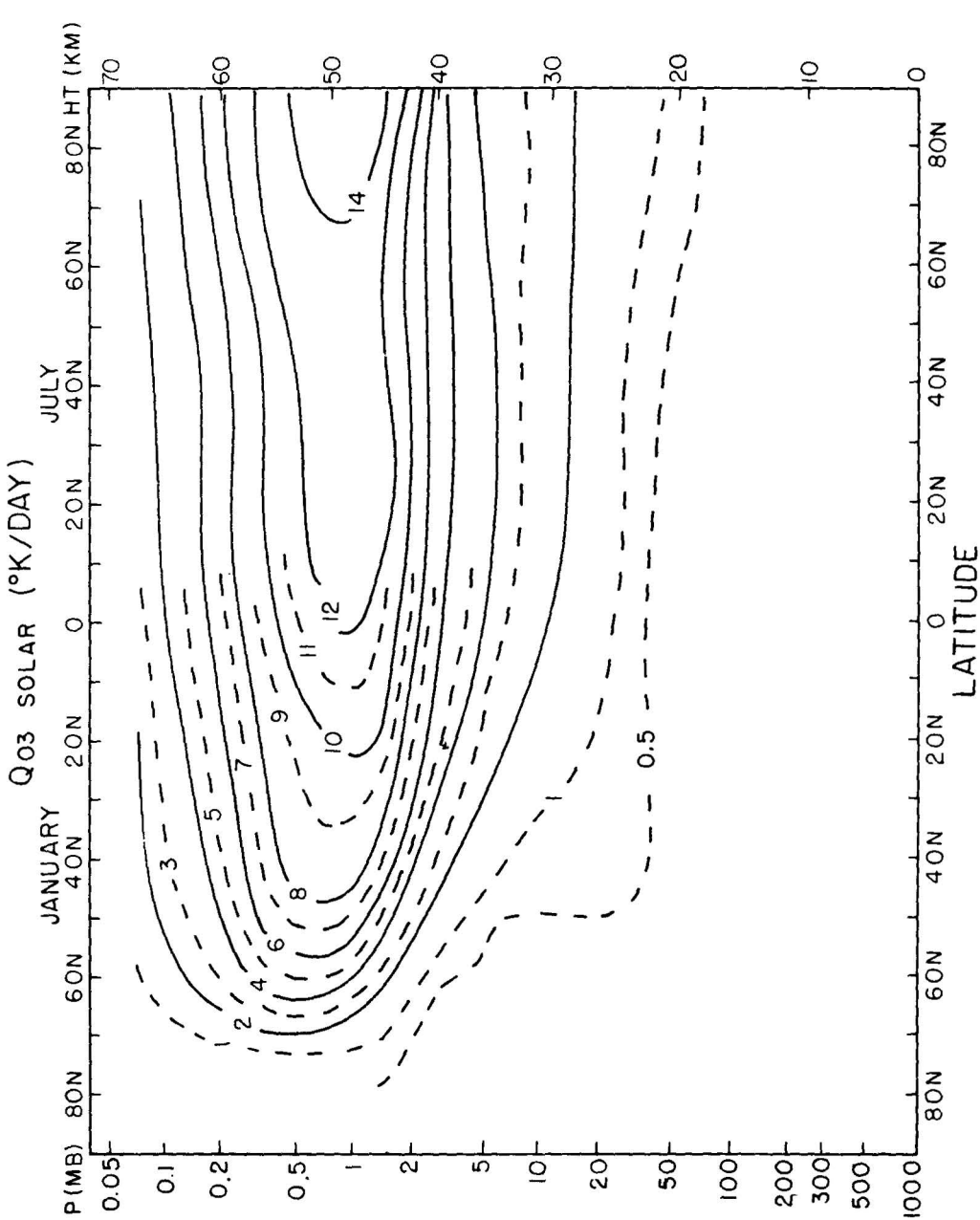


Figure 10. Radiative heating rate components (in  $^{\circ}\text{K day}^{-1}$ ) due to solar heating by ozone and infrared cooling by ozone and carbon dioxide for January and July.

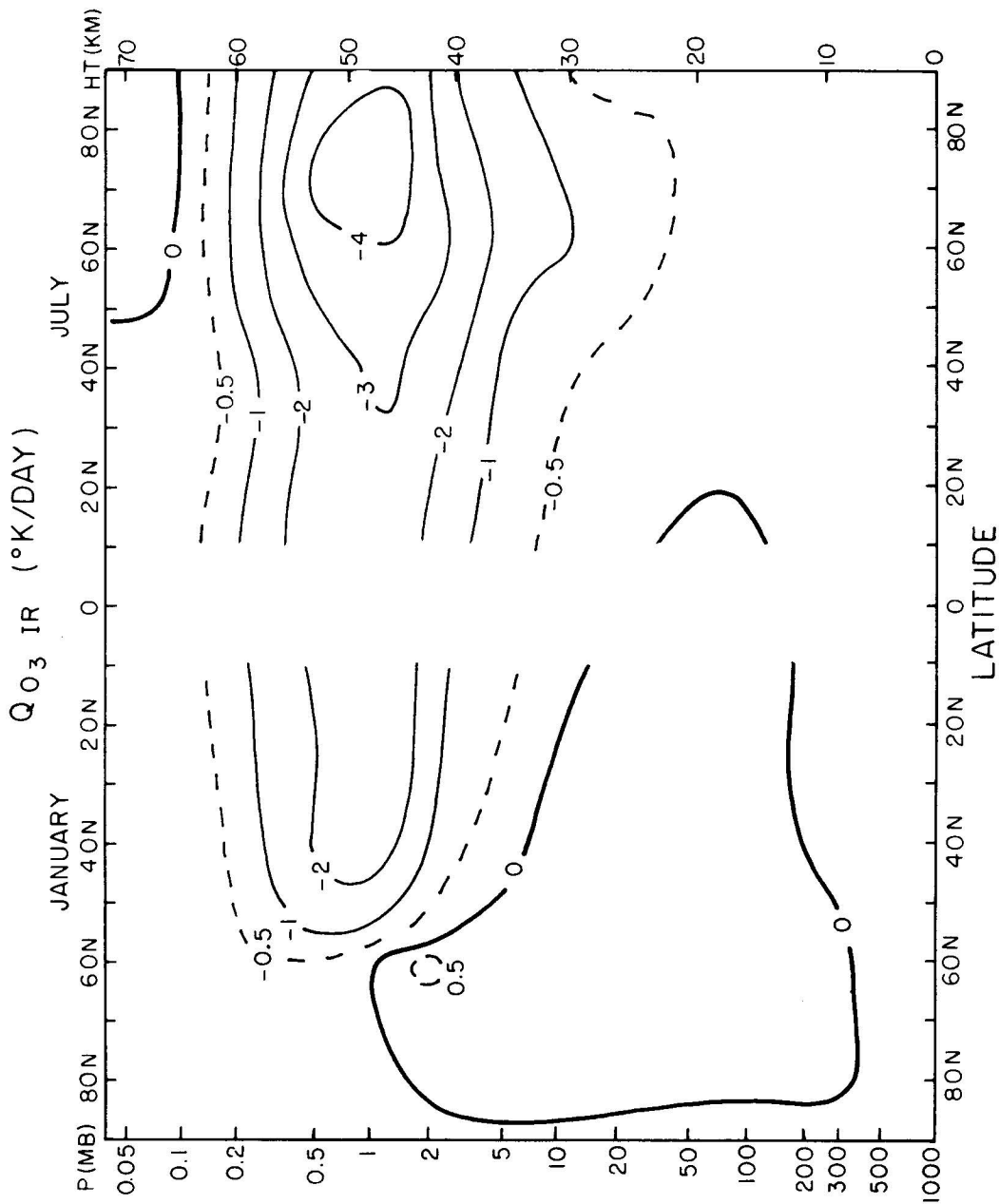


Figure 10. Continued.

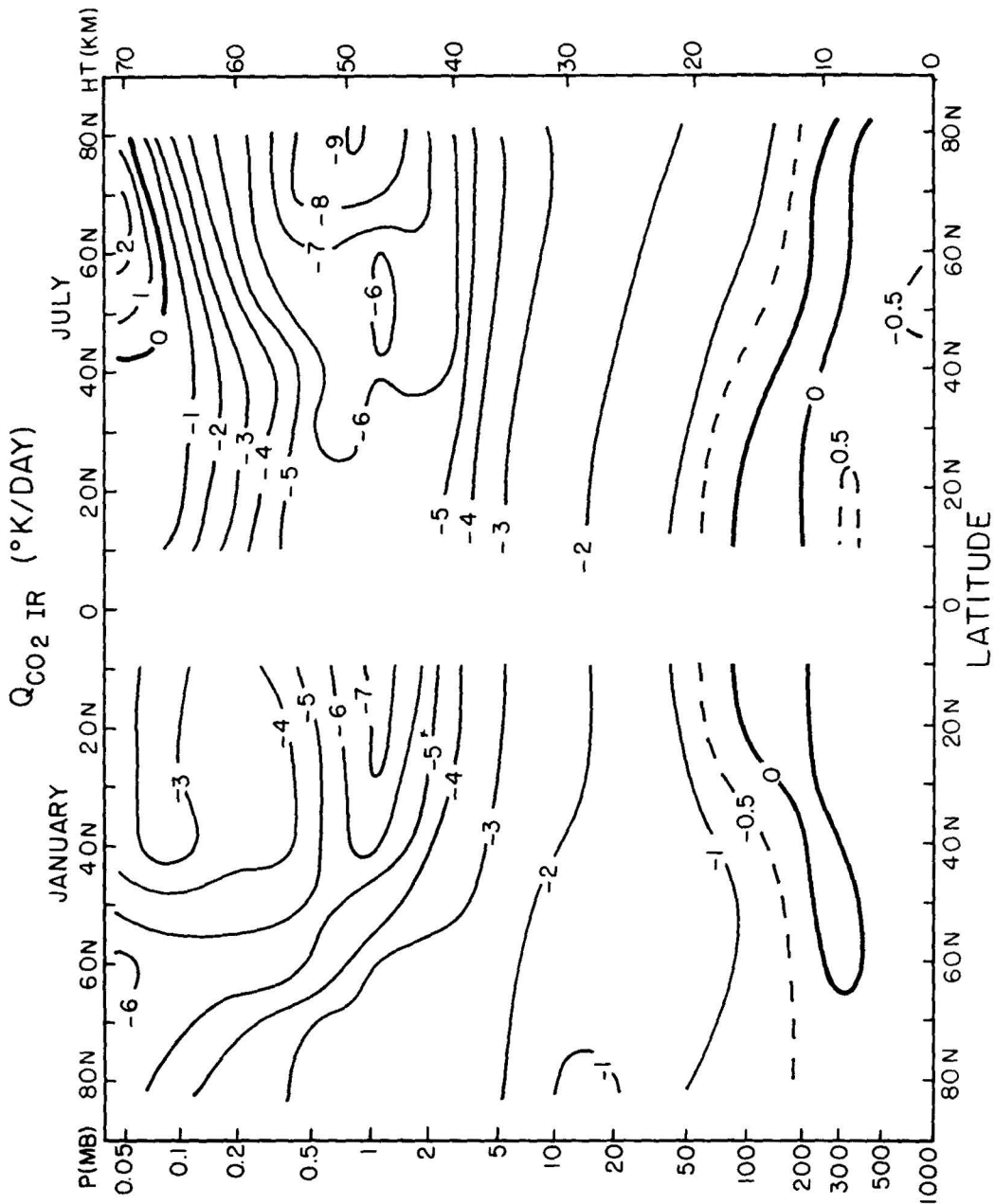


Figure 10. Continued.

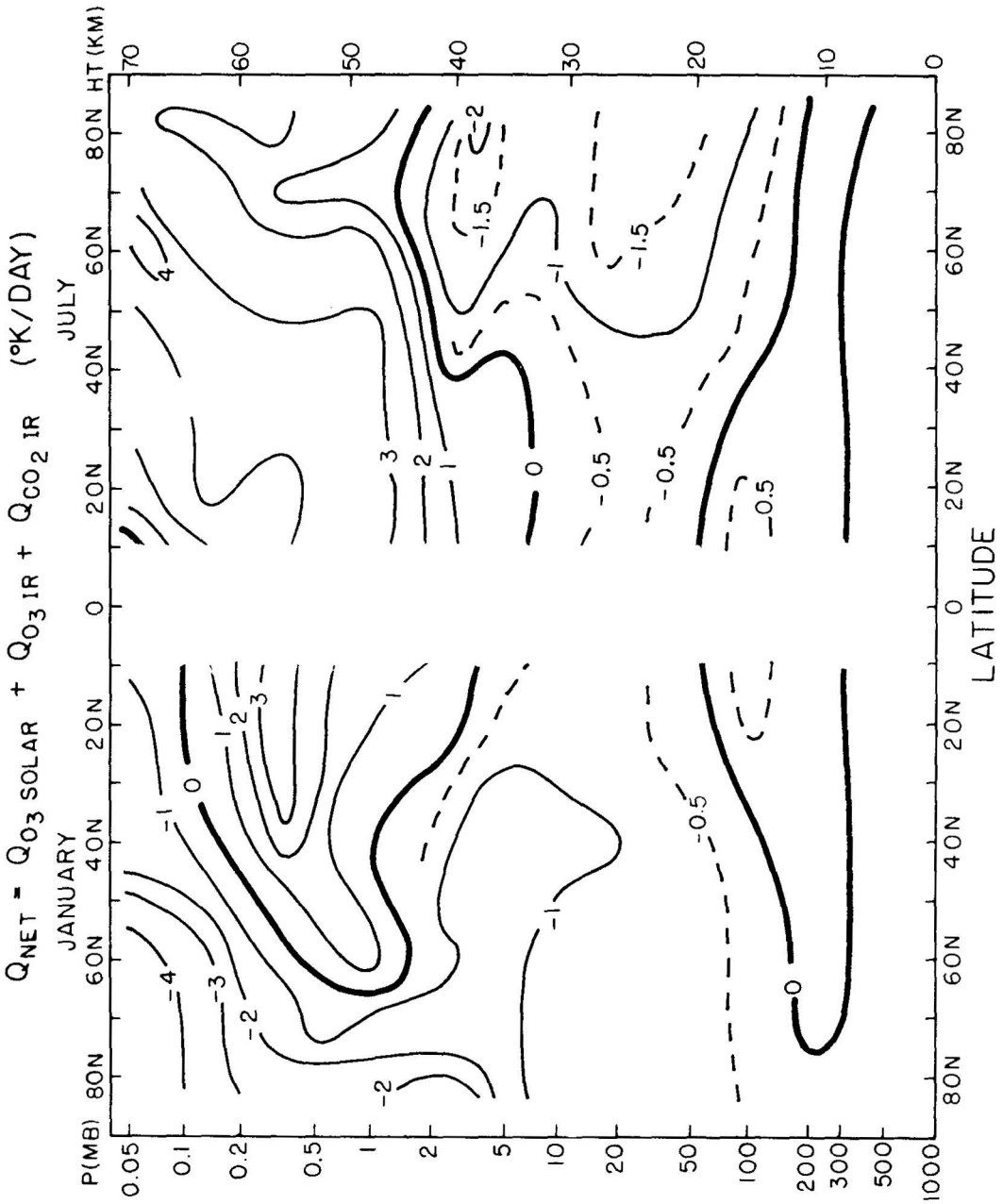


Figure 11. Net radiative heating rate from sum of components (in  $^\circ K \text{ day}^{-1}$ ) for January and July.

10 - 2 MB LAYER

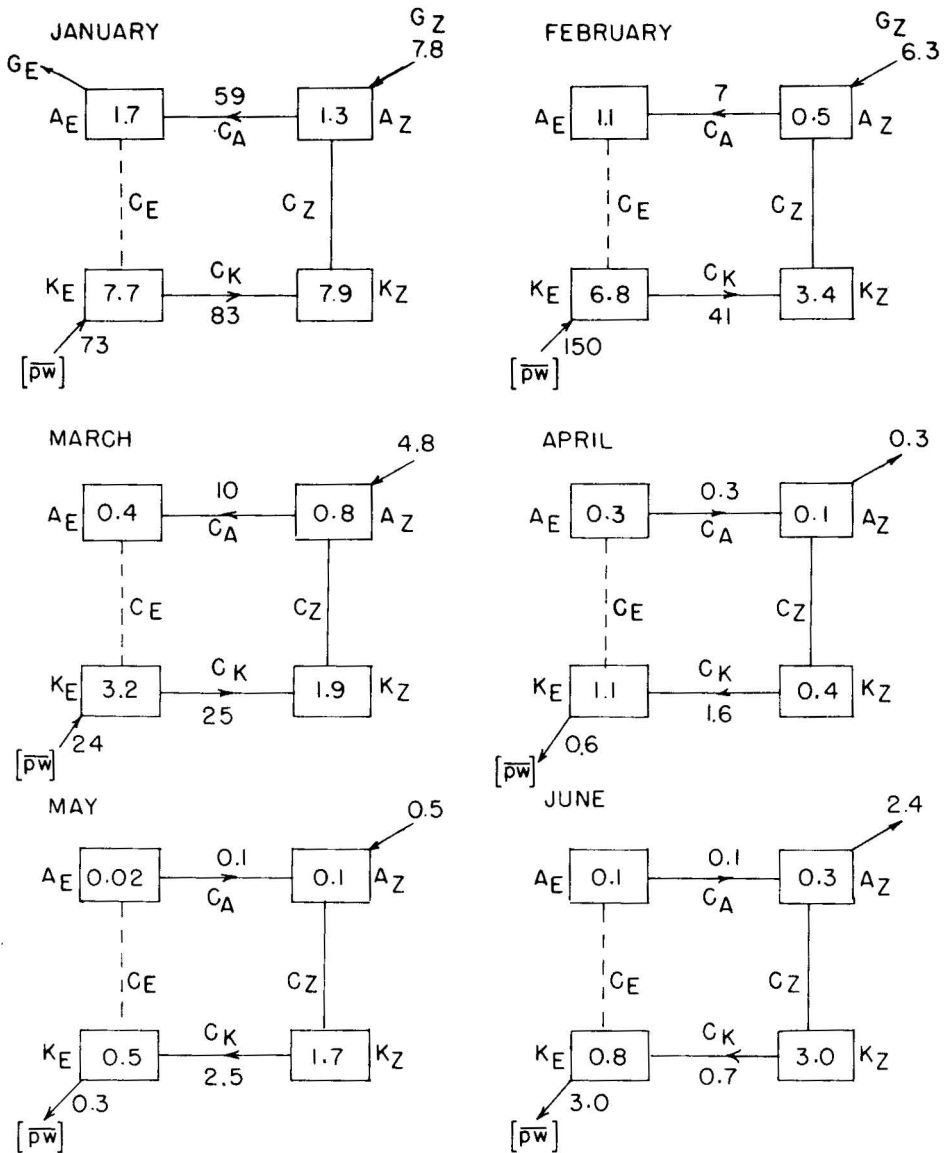


Figure 12. Energy budget components for the 10-2 mb layer for each month. Units: Contents in  $10^{25}$  ergs, and conversion rates in  $10^{18}$  ergs  $\text{sec}^{-1}$ .

### 10 - 2MB LAYER

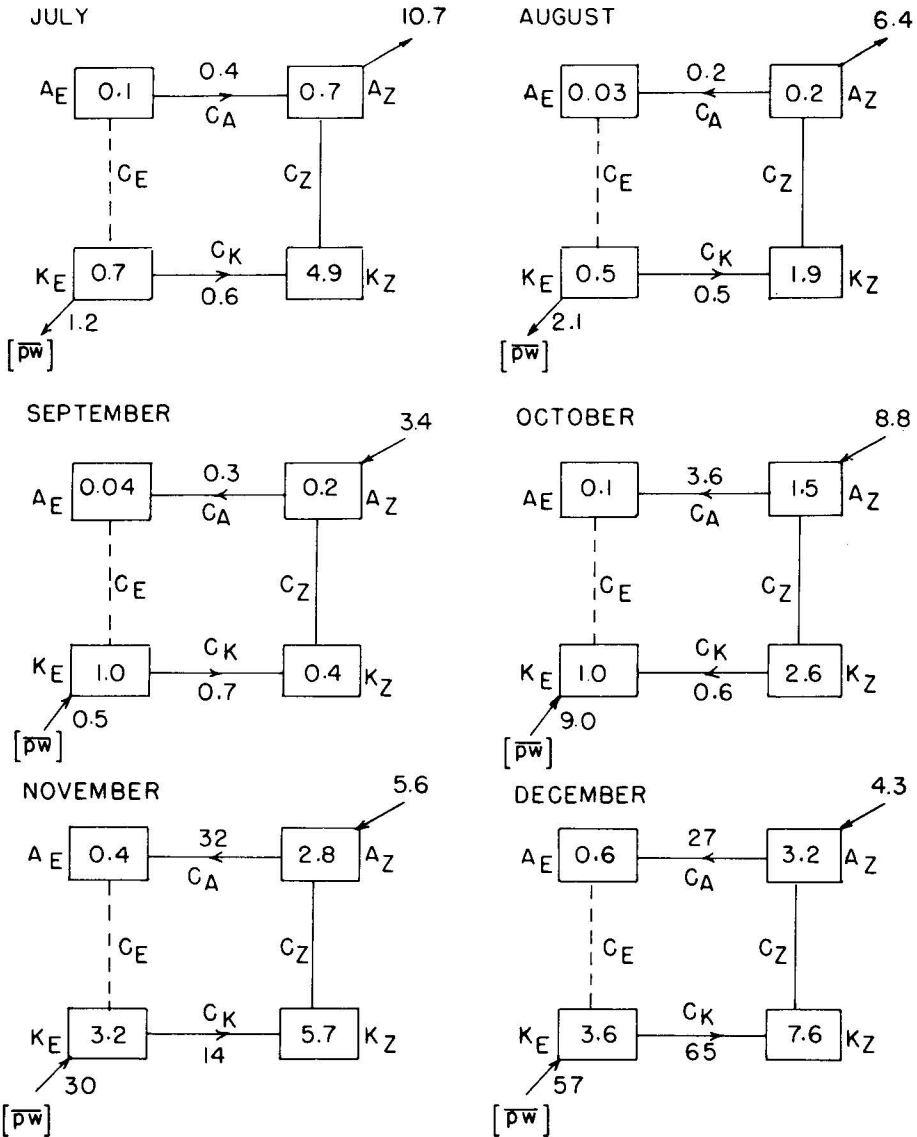


Figure 12. Continued.

## BIBLIOGRAPHY

- BOVILLE, B. W., 1961 A dynamical study of the 1958-59 stratospheric polar vortex, in *Meteorology* No. 36, Arctic Meteorology Research Group, McGill University, Montreal. 134 pp.
- CHARNEY, J. G. and P. G. DRAZIN, 1961. Propagation of planetary scale disturbances from the lower into the upper atmosphere, *J. Geophys. Res.*, 66: 83-109.
- CRUTCHER, H. L. and J. M. MESERVE, 1970. Selected level heights, temperatures and dew points for the northern hemisphere, *NAVAIR 50-IC-52*, Naval Weather Service Command, Washington, D. C.
- CUNNOLD, D., F. ALYEA, N. PHILLIPS and R. PRINN, 1975. A three-dimensional dynamical-chemical model of atmospheric ozone, *J. Atmos. Sci.*, 32:170-194.
- DELAND, R. J., 1973. Analysis of Nimbus 3 SIRS Radiance data: travelling planetary-scale waves in the stratospheric temperature field, *Monthly Weather Review*, 101:132-140.
- DOPPLICK, T. G., 1971. The energetics of the lower stratosphere including radiative effects, *Quart. J. Roy. Met. Soc.*, 97:209-237.
- ELIASSEN, A. and E. PALM, 1961. On the transfer of energy in stationary mountain waves, *Geof. Pub.*, XXII, 23 pp.
- GROVES, G. V., 1971. Atmospheric structure and its variations in the region from 25 to 125 km, Air Force Cambridge Res. Labs., *Report No. 71-0410*, Bedford, Mass.
- HIROTA, I. and Y. SATO, 1969. Periodic variation of the winter stratospheric circulation and intermittent vertical propagation of planetary waves, *J. Met. Soc. Jap.*, 47:390-402.
- LABITZKE, K., K. PETZOLDT, B. NAUJOKAT, E. KLINKER and R. LENSCHOW, 1975. The stratospheric midwinter warming during December 1974-January 1975, *Beilag zur Berliner Wetterkarte*, Frei Univ. Berlin, 12 pp.
- LORENZ, E. N., 1955. Available potential energy and the maintenance of the general circulation, *Tellus*, 7:157-167.
- MILLER, A. J., J. A. BROWN and K. A. CAMPANA, 1972. A study of the energetics of an upper stratospheric warming (1969-70), *Quart. J. Roy. Met. Soc.*, 98:730-744.
- MUENCH, H. S., 1965. On the dynamics of the wintertime stratospheric circulation, *J. Atmos. Sci.*, 22:349-360.
- NEWELL, R. E., 1963. Preliminary study of quasi-horizontal eddy fluxes from Meteorological Rocket Network data, *J. Atmos. Sci.*, 20:213-225.
- NEWELL, R. E., 1964a. Further ozone transport calculations and the spring maximum in ozone amount, *Pure and Applied Geophysics*, 59:191-206.
- NEWELL, R. E., 1964b. Stratospheric energetics and mass transport, *Pure and Applied Geophysics*, 58:145-156.
- NEWELL, R. E. and M. E. RICHARDS, 1969. Energy flux and convergence

- patterns in the lower and middle stratosphere during the IQSY, *Quart. J. Roy. Met. Soc.*, 95:310-328.
- NEWELL, R. E., J. W. KIDSON, D. G. VINCENT and G. J. BOER, 1972. *The General Circulation of the Tropical Atmosphere*, Vol 1, The M.I.T. Press, Cambridge, Mass., 258 pp.
- NEWELL, R. E., G. F. HERMAN, J. W. FULLMER, W. R. TAHNK and M. TANAKA, 1974a. Diagnostic studies of the general circulation of the stratosphere. *Proceedings: International Conference on structure, composition and general circulation of the upper and lower atmospheres and possible anthropogenic perturbations held in Melbourne, Australia, January 1974*, Office of the Secretary, IAMAP, Atmosphere Environment Service, Canada, Vol. I, pp. 17-82.
- NEWELL, R. E., J. W. KIDSON, D. G. VINCENT and G. J. BOER, 1974b. *The General Circulation of the Tropical Atmosphere*, Vol. 2, The M.I.T. Press, Cambridge, Mass., 371 pp.
- OORT, A. H. and E. M. RASMUSSEN, 1971. Atmospheric Circulation Statistics, *Prof. Paper No. 5*, NOAA, U. S. Dept. of Commerce, Rockville, Md., 323 pp.
- OXFORD UNIVERSITY, DEPT. OF ATMOSPHERIC PHYSICS, 1972. *Global Stratospheric Analyses*, Oxford Press, Oxford, Eng., 109 pp.
- QUIROZ, R. S., 1975. The stratospheric evolution of sudden warmings in 1969-74 determined from measured infrared radiation fields, *J. Atm. Sci.*, 32:211-224.
- RICHARDS, M. E., 1967. The energy budget of the stratosphere during 1965, *Report No. 21*, Planetary Circulations Project, Dept. of Meteor., M.I.T., 171 pp.
- SATO, Y., 1974. Vertical structure of quasi-stationary planetary waves in several winters, *J. Met. Soc. Jap.*, 52:272-281.
- SIMMONS, A. J., 1974. Planetary-scale disturbances in the polar winter stratosphere, *Quart. J. R. Met. Soc.*, 100:76-108.
- SLADE, W. J., JR., 1975. Infrared cooling of the atmosphere by the 9.6 micron band of ozone, *SM Thesis*, Massachusetts Institute of Technology, Cambridge, Mass., 75 pp.
- STAFF, UPPER AIR BRANCH NMC, 1975. Synoptic analyses, 5-, 2- and 0.4 millibar surfaces for January 1972 through June 1973, *NASA SP-3091*, NASA, Washington, D. C., 205 pp.
- TAHNK, W. R., 1973. The energy budget of the middle and upper stratosphere, *SM Thesis*, Massachusetts Institute of Technology, Cambridge, Mass., 116 pp.
- TEWELES, S., 1963. Spectral aspects of the stratospheric circulation during the IGY, *Report No. 8*, Planetary Circulations Project, Dept. of Meteorology, MIT, Cambridge, Mass., 191 pp.
- VAN LOON, H., R. A. MADDEN and R. L. JENNE, 1975. Oscillations in the winter stratosphere: Part I. Description, *Mon. Wea. Rev.*, 103:154-162.